Experimental Investigation of a Refrigerator with a Dual Temperature Evaporator

H. Ge and C. W. Bullard

ACRC TR-156 September 1999

For additional information:

Air Conditioning and Refrigeration Center
University of Illinois
Mechanical & Industrial Engineering Dept.
1206 West Green Street
Urbana, IL 61801

(217) 333-3115

Prepared as part of ACRC Project 66
Refrigerator Systems Analysis
C. W. Bullard, Principal Investigator

The Air Conditioning and Refrigeration Center was founded in 1988 with a grant from the estate of Richard W. Kritzer, the founder of Peerless of America Inc. A State of Illinois Technology Challenge Grant helped build the laboratory facilities. The ACRC receives continuing support from the Richard W. Kritzer Endowment and the National Science Foundation. The following organizations have also become sponsors of the Center.

Amana Refrigeration, Inc.
Brazeway, Inc.
Carrier Corporation
Chrysler Corporation
Copeland Corporation
Delphi Harrison Thermal Systems
Frigidaire Company
General Electric Company
Hill PHOENIX
Honeywell, Inc.
Hussmann Corporation
Hydro Aluminum Adrian, Inc.
Indiana Tube Corporation
Lennox International, Inc.
Modine Manufacturing Co.
Parker Hannifin Corporation
Peerless of America, Inc.
The Trane Company
Thermo King Corporation
Visteon Automotive Systems
Whirlpool Corporation
York International, Inc.

For additional information:

Air Conditioning & Refrigeration Center
Mechanical & Industrial Engineering Dept.
University of Illinois
1206 West Green Street
Urbana IL 61801

217 333 3115

Table of Contents

List of Tables

List of Figures

Chapter 1 Introduction

Abstract

A prototype refrigerator/freezer was fitted with a single evaporator, ducted so it could serve both compartments in a sequential manner. Two capillary tubes, one optimized for each compartment were attached to the suction line and controlled by a solenoid valve. A two-speed compressor operated at 3600 rpm in freezer mode and 2400 rpm when serving the food compartment. A variable speed fan was used to explore the response of the evaporator. The experimental results confirmed earlier simulation analyses, which predicted that achieving maximum energy savings (approx. 15%) would require a two-speed compressor having a high/low speed ratio of 5.

1.1 Introduction

A "dual-temperature" evaporator refrigerator means a sequential cycle, single-evaporator refrigerator system. In this type of refrigerator, the same evaporator is sequentially used first to cool the freezer compartment and then the fresh food compartment. The air flow over the evaporator coil is directed into one compartment at a time, and is switched back and forth.

The major advantage of a dual-temperature evaporator system is that while the refrigerator is running in the fresh food mode, the lower temperature lift in the evaporator can increase the steady state COP by nearly a factor of two. Theoretically, since the fresh food compartment represents about one-third of the total evaporator load and the operating efficiency in this mode can be nearly doubled, the overall system COP might be reduced by as much as 15-20%. Furthermore, if the system is optimized for each compartment separately, the COP in the freezer mode can be also enhanced by using a different capillary tube or varying the compressor speed.

An additional performance improvement might result from using the relatively warm fresh food compartment air to defrost the evaporator during the off-cycle. This could greatly decrease, or possibly eliminate the auxiliary power requirements entirely, reducing the system complexity, its initial cost, and overall energy usage. In this respect the sequential cycle single-evaporator system has an advantage over dual-evaporator systems which need heaters to defrost the freezer coil.

The disadvantage of this single-evaporator approach is the need for a solenoid valve to switch refrigerant flow between two capillary tubes; one optimized for freezer operation, the other for fresh food mode. In addition, there is a reliability risk associated with the air damper mechanism. We used a simple motor-driven prototype donated by Siebe Appliance Controls. Finally as Kelman and Bullard (1999) concluded during the design phase, a variable- or multi-speed compressor with a 5:1 turndown ratio would be needed in order to maximize energy savings obtainable from this technology.

1.2 Purpose

Kelman and Bullard (1999) designed a dual-temperature evaporator refrigerator prototype on the basis of an existing 25 cubic foot, side-by-side Amana refrigerator, and analyzed the system performance by using an ACRC refrigerator simulation model, developed by Woodall and Bullard (1996, 1997) and carefully validated using data from the original system equipped with a single-speed compressor.

The experimental work described in this report is performed on the prototype designed by Kelman. The capillary tube lengths and system charge were optimized experimentally for both freezer mode and fresh food mode on the criterion of highest COP, suitable condenser subcooling and evaporator superheat. The system performance of the optimized refrigerator was tested and analyzed at the standard Department of Energy test conditions. The additional experiments were also conducted over a range of evaporator fan speeds, to understand the different evaporator performances with variable-speed evaporator fan at dual evaporating temperatures.

1.3 Prototype refrigerator

The experimental refrigerator was originally a 25 ft^3 side-by-side Amana refrigerator, model SRD25S5W, with a factory suggested 5.125 ounces of R-134a. It was extensively modified to be a dual-temperature evaporator refrigerator system (details in Appendix A).

The original single speed Tecumseh compressor, Model TP1390YXA, was replaced with a multi-speed Ameritech compressor, Model RV670-1. Using accelerometers mounted on the compressor shell (same method was described by Srichai and Bullard, 1997), the compressor

speed was adjusted and operated at either 1890 rpm for fresh food mode or 3750 rpm for freezer mode, with a turndown ratio of approximately 2.0.

The original evaporator was replaced by a re-designed one, and installed at a different location, in the rear of the fresh food compartment. The air flow across the evaporator can be drawn from and directed into either freezer compartment or fresh food compartment through a specially designed switched system.

The original capillary tube was replaced with 4 tubes having different lengths and diameters to allow choices during optimization procedures at both modes.

Chapter 2 System Performance Analysis

2.1 Introduction

Capillary tubes were cut and charge was adjusted to optimize COP in both freezer mode and fresh food mode with the evaporator fan at its maximum speed (see Appendix D); then tests were conducted to see how the evaporator air-side heat transfer affects the system performance.

Evaporator heat transfer characteristics are very important to the refrigerator's overall performance. Especially the air-side heat transfer, which consists most of the heat transfer resistance, contributes significantly to the evaporator performance.

From our test in the fresh mode optimization, we found that a high superheat in the evaporator exit existed even when the subcooling satisfied the optimization criterion, because the capillary tube diameter was too small and its length was at its minimum. One possible Therefore during our tests we reduced the evaporator fan speed to increase the wetted are of the evaporator and to examine the tradeoff between fan and compressor power as they affect COP. The evaporator fan used here is a variable fan manufactured by Nidec (model TA500DC). It is rated at 150 cfm by manufacturer while operating at its maximum speed at 48 Volts DC. Lower speeds were achieved by turning the voltage down.

2.2 Freezer mode

In freezer mode, our optimization criterion is to seek both 5 °F subcooling and 5 °F superheat, so there is only moderate superheat at the evaporator exit. Tests were conducted by decreasing the input voltage by one-volt increments until the superheat disappeared. Table 1 shows the system performance as air flow rates were varied. Here, the air flow rates were calculated through dividing the cooling capacity, excluding the evaporator fan power, by the air side enthalpy change across the evaporator. The difference between the evaporator air outlet temperature and refrigerant outlet temperature is designated $\Delta T_{approach}$.

Evap. Fan Volt (VDC)	EvapFan Power (W)	Tr_sat: CondOut (°F)	Tr_sat: EvapOut (°F)	Air flow rate (cfm)	Sub-cooling (°F)	Super-heat (°F)	COP	Cooling Cap. (W)	ΔT approach (°F)
47.8	10.8	106.3	-16.4	48.74	13.5	10.4	1.20	217.3	-0.5
47	10.4	106.1	-16.6	47.42	13.3	10.2	1.20	217.7	-0.3
46	9.9	106.0	-16.6	46.28	13.2	9.6	1.21	218.6	0.1
45	9.4	105.7	-16.7	44.78	13.0	8.1	1.23	217	1.4
44	9.0	105.7	-15.4	43.41	6.0	2.0	1.19	212.8	6.2

Table 2.1 Freezer system performance with variable fan speeds

Table 2.1 shows that the system COP and capacity are relatively insensitive to the evaporator fan speed. Apparently the decrease in air side heat transfer coefficient offset the increase in two-phase heat transfer area, as superheat was reduced from about 10°F to 2°F.

2.3 Fresh food mode

Evap Fan Volt (VDC)	EvapFan Power (W)	Tr_sat: CondOut (°F)	Tr_sat: EvapOut (°F)	Air flow rate (cfm)	Sub-cooling (°F)	Super-heat (°F)	COP	Cooling Cap. (W)	Runtime fraction
47.8	10.5	109.8	16.1	50.29	5.1	27.6	1.86	262.9	0.056
45	9.2	109.4	15.7	48.08	4.8	27.9	1.89	261.7	0.055
42	7.9	109.0	15.3	45.37	4.4	27.7	1.91	258.4	0.055
39	6.7	108.7	14.9	42.6	4.1	26.6	1.93	256.4	0.055
36	5.5	108.8	14.8	39.36	3.2	22.8	1.94	254.8	0.056
33	4.5	108.9	14.7	36.44	2.1	18.4	1.95	252.8	0.057
30	3.6	107.6	13.1	33.09	2.3	20.9	1.95	244.4	0.056
25	2.3	107.3	12.4	27.29	1.0	13.6	1.91	233.9	0.059
22	1.7	106.9	11.3	22.84	0.2	6.1	1.89	225.7	0.062
20	1.2	106.2	9.4	20.04	0.1	2.7	1.82	210.8	0.066

Table 2.2 Fresh food system performance with variable fan speeds

Since refrigerant charge was fixed during freezer mode optimization, superheat during fresh food mode optimization reached 27 °F as we approached the 5°F subcooling constraint while optimizing COP for the fresh food mode. Therefore we could expect that variable fan speed would affect the system a lot more significant than freezer mode. Table 2 shows the system performance for fresh food mode with variable evaporator fan speed. Here the runtime fraction was calculated as the following: First the real heat load at the DoE standard condition was calculated using the UA values found for this refrigerator (see Appendix C); then this heat load was divided by the cooling capacity to get the runtime fraction. Reverse heat leak tests

were conducted with the fan on, and indicated that the mullion UA was degraded about 50% due to imperfect sealing around the dampers.

Figure 2.1 shows how subcooling and superheat varied with the evaporator air flow rate. Both subcooling and superheat decreased as the fan speed reduced.

Fig. 2.1 Subcooling and Superheat vs. Fan Air Flow Rate

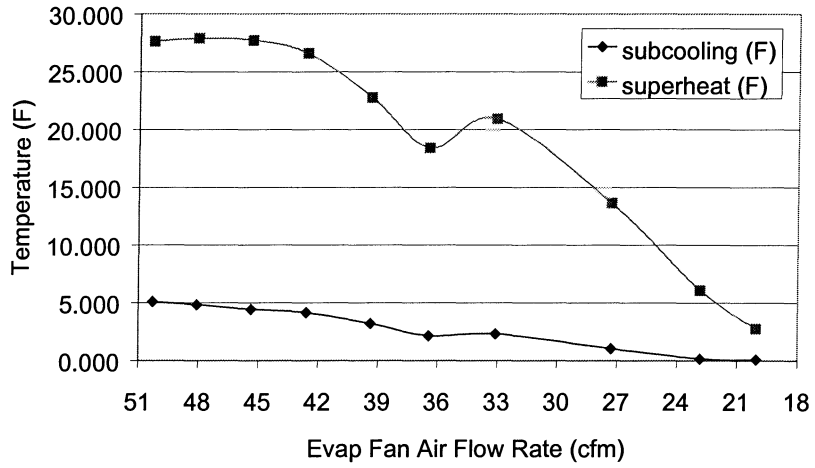

Figure 2.2 and 2.3 show the change of system pressures with evaporator fan speed. Both pressures decreased as the fan speed was reduced.

Fig. 2.2 Condensing Temp. vs. Evap Fan Air Flow Rate

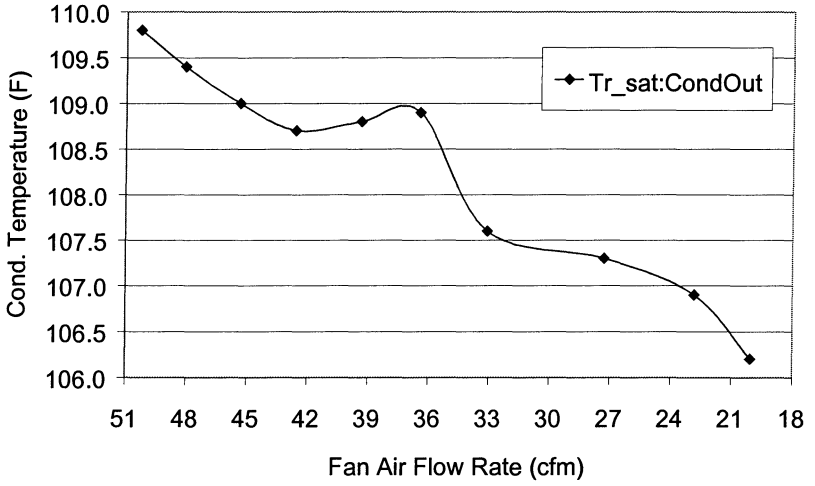

Fig. 2.3 Evaporating Temp. vs. EvapFan Air Flow Rate

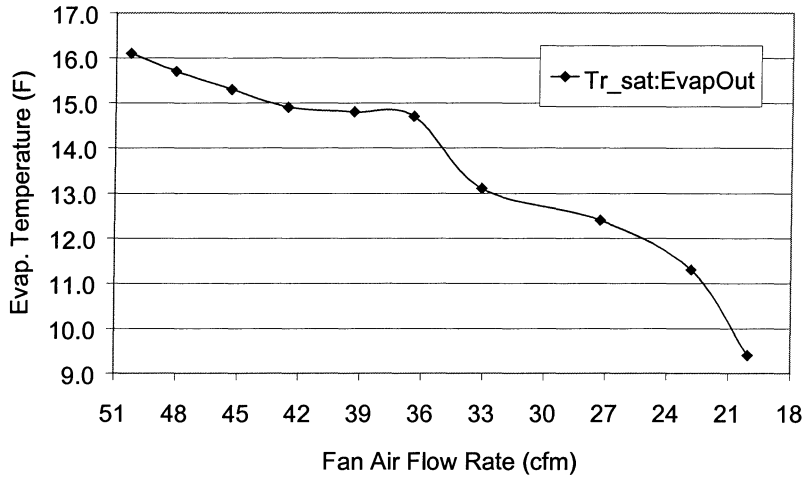

Fig. 2.4 COP vs. EvapFan Air Flow Rate

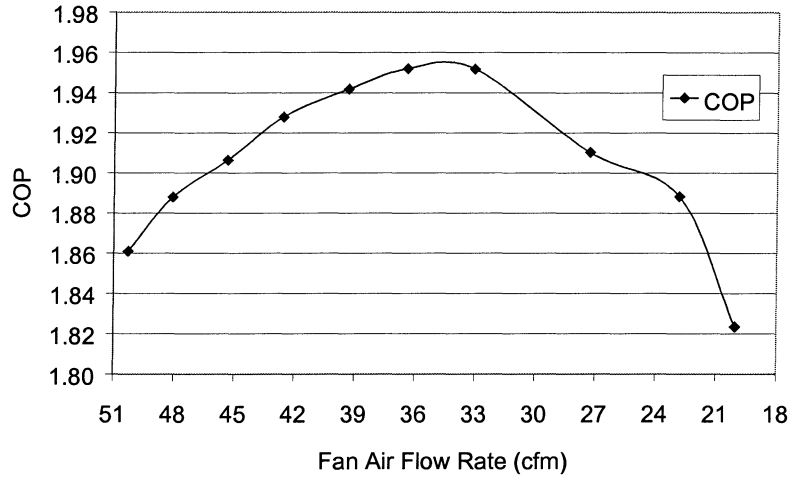

Fig. 2.5 Cooling Capacity vs. EvapFan Air Flow Rate

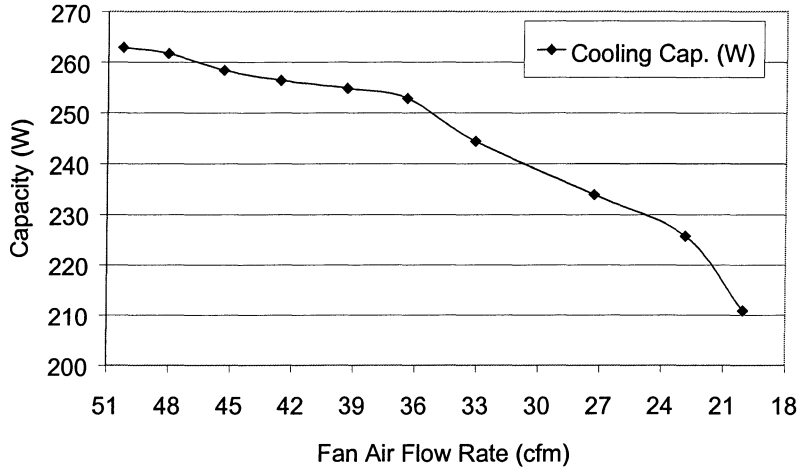

Fig. 2.6 FFC Runtime Fraction vs. EvapFan Air Flow Rate

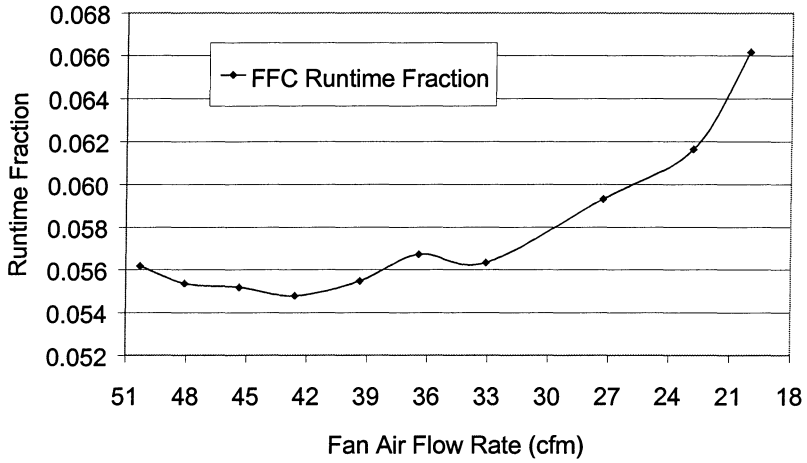

Figure 2.4 - 2.6 show the COP, cooling capacity and runtime fraction change with the evaporator fan speed. The COP first increased then decreased as the fan speed reduced, and the highest COP achieved at about 35 cfm. The cooling capacity decreased as the fan speed was reduced, which caused the runtime fraction to increase. The runtime fraction for the fresh food compartment is still quite low, and could exacerbate cycling losses instead of reducing them. However if the compressor turndown ratio were 5:1 instead of 2:1 there would be no problem.

Had the fresh food compartment's captube diameter been slightly larger (or its length shorter) there would have been no need to turn down the fan speed in fresh food mode. In our case due to the 2:1 turndown ratio, a lower fan speed actually helped improve runtime fraction. In an optimized system, the tradeoff would be between noise and energy efficiency.

As both higher COP and higher runtime fraction are favorable to fresh food operation, the best evaporator fan speed for this prototype should produce an air flow rate of 33-36 cfm. Since fan power varies nonlinearly with the air flow rate, it is possible to achieve quieter operation in fresh food mode.

2.4 COP and runtime fraction

	COP		Runtime fraction	
	simulation	test	simulation	test
Freezer Mode	1.05	1.20	0.54	0.59
Fresh Food Mode	1.86	1.95	0.17	0.06

Table 2.3 COP and Runtime fraction for freezer and fresh food

Table 2.3 shows the best COP and runtime fraction achieved in our test, compared with the simulation results by Kelman (1999). The simulation model had been verified at a compressor speed of 3600 rpm. The experimental results for freezer mode (the compressor speed was set to 3600 rpm) showed that system performance exceeded the prediction by 15 %. However, the simulation results for fresh food mode (the compressor speed was set to be 1800 rpm) the COP test results were much closer to the predicted values. The runtime data demonstrates confirms that there was substantial heat leakage through the relatively crude dampers separating the two compartments of our prototype. This led to a steady heat loss of about 30W to the freezer, compared to the 45W heat gain through the exterior walls of the fresh food compartment. This reduced the fresh food compartment load by a factor of 3, and shortened runtime accordingly. Mullion heat transfer is therefore one of the factors that needs to be addressed in the design of such systems. From our test results, the fresh food mode COP is over 60% higher than the freezer mode. Generally, the fresh food heat load is about one-third of the total refrigerator heat load. If this portion of heat load was removed under almost steady-state fresh food mode operation, we could get a nearly 15% higher overall average COP by using the dual temperature evaporator system, compared to the ordinary refrigerator.

But this COP benefit might be greatly undermined by frequent on-off cycles in fresh food cooling for the real refrigerator, especially when we have a small fresh food runtime fraction as with our test prototype (the fresh food runtime fraction was only 5.7%).

The turndown ratio of compressor used in our test was limited to a factor of 2.0. Using turndown ratios higher than 2.0 could increase both COP and runtime fraction for fresh food mode, thus result in greater energy savings. But it might cause lubrication problems, which could lead to poor reliability. However, some prototype units that are currently being tested by some

manufacturers might have turndown ratios as high as 6.0. If this kind compressor are used in the dual temperature evaporator refrigerator, a much higher COP and better on-off cycle performance can be achieved.

References

Kelman, S., "Dual Temperature Evaporator Refrigerator Design and Optimization," ACRC TR-148, University of Illinois at Urbana-Champaign, 1999.

Srichai, P.R. and C.W. Bullard, "Two-Speed Compressor Operation in a Refrigerator/Freezer," ACRC TR-121, University of Illinois at Urbana-Champaign, 1997

Woodall, R.J., and C. W. Bullard, "Simulating effects of variable speed compressor on refrigerator/freezer performance," ASHRAE Transactions, 103:2, 630-639, 1997.

Appendix A

System Modification and Instrumentation

The experimental refrigerator was originally a 25 ft^2 side-by-side Amana refrigerator, model SRD25S5W, with a factory suggested 5.125 ounces of R-134. It was heavily modified to be a dual-temperature evaporator refrigerator system.

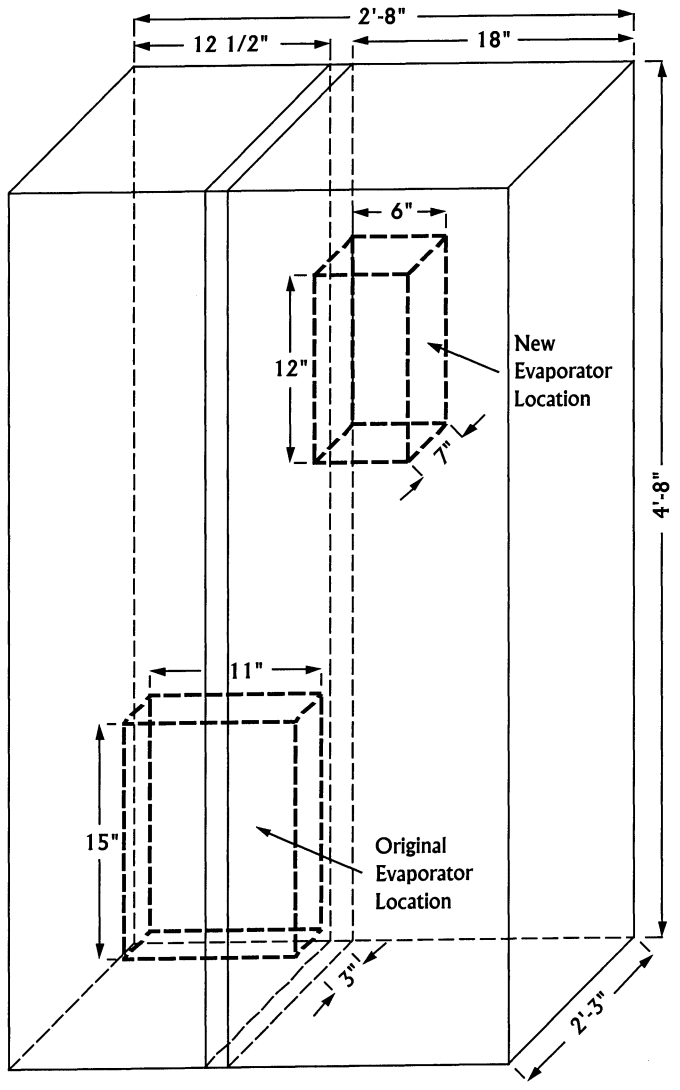

Figure A.1 Evaporator location diagram

The original single speed Tecumseh compressor, Model TP1390YXA, was replaced with a multi-speed Ameritech compressor, Model RV670-1. The compressor speed was adjusted and

operated at either 1890 rpm for fresh food mode or 3750 rpm for freezer mode, with a turn down ratio of approximate 2.0.

The original evaporator was replaced by a re-designed one, and installed at a different location, as shown in Figure A.1. The air flow across the evaporator can be drawn from and directed into either freezer compartment or fresh food compartment through a specially designed switched system, as shown in Figure A.2.

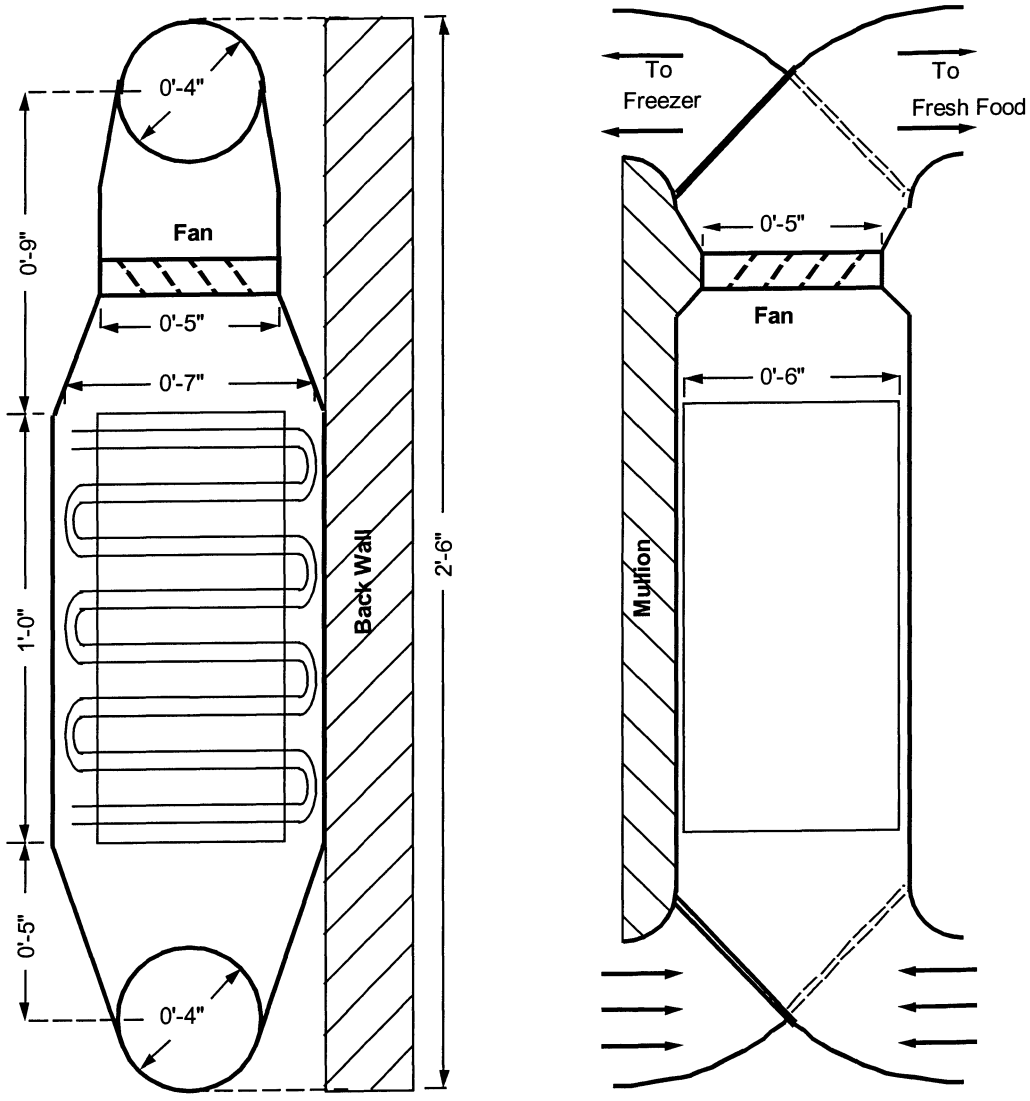

Figure A.2 Evaporator coil and ductwork diagram

The dual-temperature evaporator system has very dissimilar operating conditions while cooling the freezer or the fresh food compartments and has to be separately optimized for each

mode. One way of making sure that the system operates efficiently in both modes is by varying the compressor operating speed at a turndown ratio more than 5 (Kelman, 1999), which is still in test stage by various manufacturers. However, the compressor selected for the prototype refrigerator, has an inadequately limited turndown (less than 2.0).

This means that even by turning the compressor down to the minimum operating speed during the fresh food mode operation, it would not be possible to bring the refrigerant mass flow rate down low enough to match the mass flow rate of the system operating in the freezer mode at full compressor speed. In order to deal with different flow rates in each mode, separate capillary tubes were used exclusively during freezer as opposed to fresh food cooling.

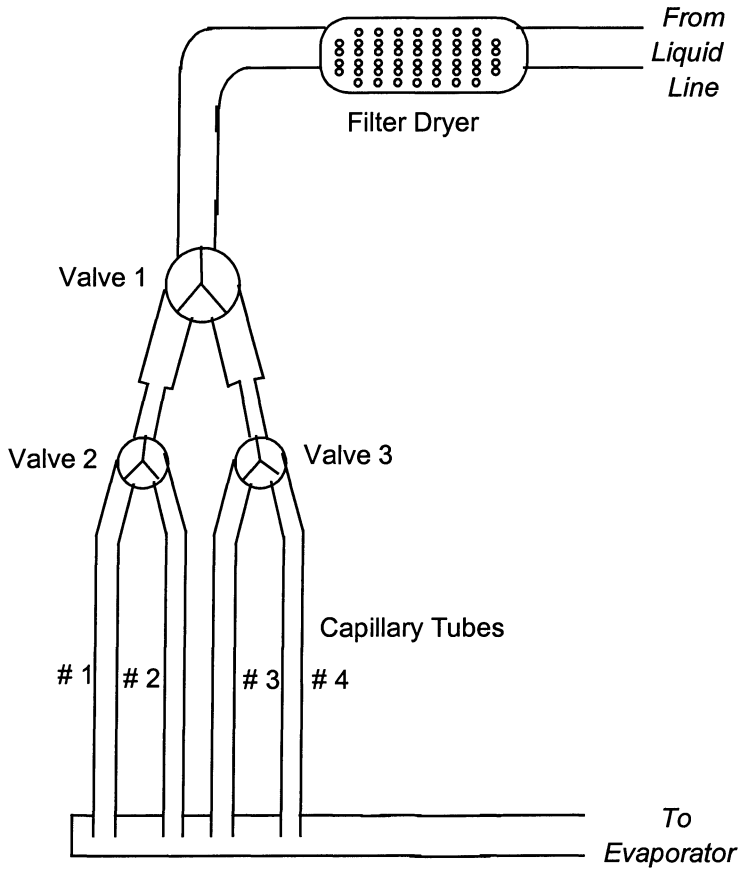

Figure A.3 Capillary tubes configuration

An inexpensive solenoid valve can be used to switch the refrigerant flow at the same time as the air valves redirect the air flow. In the future, as compressors with wider range of operating

speeds become available, the requirement for having two separate capillary tubes can be eliminated.

The original capillary tube was replaced with 4 different length and diameter capillary tube to allow choices during optimization procedures at both modes, as shown in Figure A.3. Three Y-valves were used to direct the refrigerant flow into different capillary tubes. The first and second captubes had internal diameter of 0.028 inches and initial lengths of 10 feet each. The third captube was the same length but measured 0.031 inches in diameter. Finally, the fourth captube was even thicker, being rated at 0.040 inches ID and longer, having 12 feet in length.

On one side, all of them were connected to a header that resided inside the freezer compartment. On the other side, they all went into a collection of solenoid valves mounted on the back of the frigerator. As they went into those valves, they were inserted and soldered inside special adapters custom made by the ME machine shop. These adapters were secured in the Gyrolock fittings that were screwed into the valves. Each time the captubes were snipped, the new ferrous were replaced inside the fittings and 3 layers of Teflon tape were wrapped around the threads to prevent the leaks.

Appendix B Refrigerator Instrumentation

B.1 Previously done instrumentation

The side-by-side Amana refrigerator was originally instrumented by Robert Srichai. The complete details and justification for the thermocouple and transducer placement were presented by Srichai and Bullard (1997).

The original instrumentation included 27 air-side thermocouples located inside the refrigerator cabinets as well as around the condenser and the evaporator ductwork. 37 refrigerant and surface thermocouples were also installed. Five of these were immersion thermocouples with a surface thermocouple installed at each of these locations as well. Among the 27 air-side thermocouples, the air-side thermocouples at the evaporator inlet and exit and both fresh food and freezer compartment where from the first batch and the air-side thermocouples on the inlet and exit of the condenser are from the second batch. The first batch of thermocouple wire was stated to have an uncertainty of ±1.8 °F while the second batch of thermocouple wires had an uncertainty of ±0.7 °F. Both were purchased from Omega Engineering.

Also, at each of the five locations that immersion thermocouples were placed, a pressure transducer was also installed. Absolute pressure was measured at the evaporator exit while gauge pressure was obtained at the compressor exit. Differential transducers were used to measure the pressure drops across the condenser, the liquid line and the suction line. The atmospheric pressure was also logged.

Finally, watt transducers were installed to measure the heater powers, the fan powers and the total system energy consumption.

B.2 New instrumentation

B.2.1 General considerations

Just like for the original thermocouples, 24 AWG type T thermocouple wire was purchased from Omega Engineering. Due to the big uncertainty (±1.8 °F) of first batch thermocouples used inside the cabinets and relocation of the evaporator and ductwork, the first batch thermocouples were totally removed and new AWP type T thermocouples, with an uncertainty of ±0.7 °F, were reinstalled inside both cabinets.

B.2.2 Air-side instrumentation

All the air-side thermocouples inside both cabinets installed by Srichai were removed and total eight new thermocouples, numbering from 1 to 8 were reinstalled inside them. In each cabinet, one thermocouple was 10" from the top of the back wall; the second was 11" from its bottom; and the last two were at the back wall center. All the thermocouple heads were 4" away from the back wall.

Condenser air-side instrumentation was left intact, only the naming numbers were rearranged.

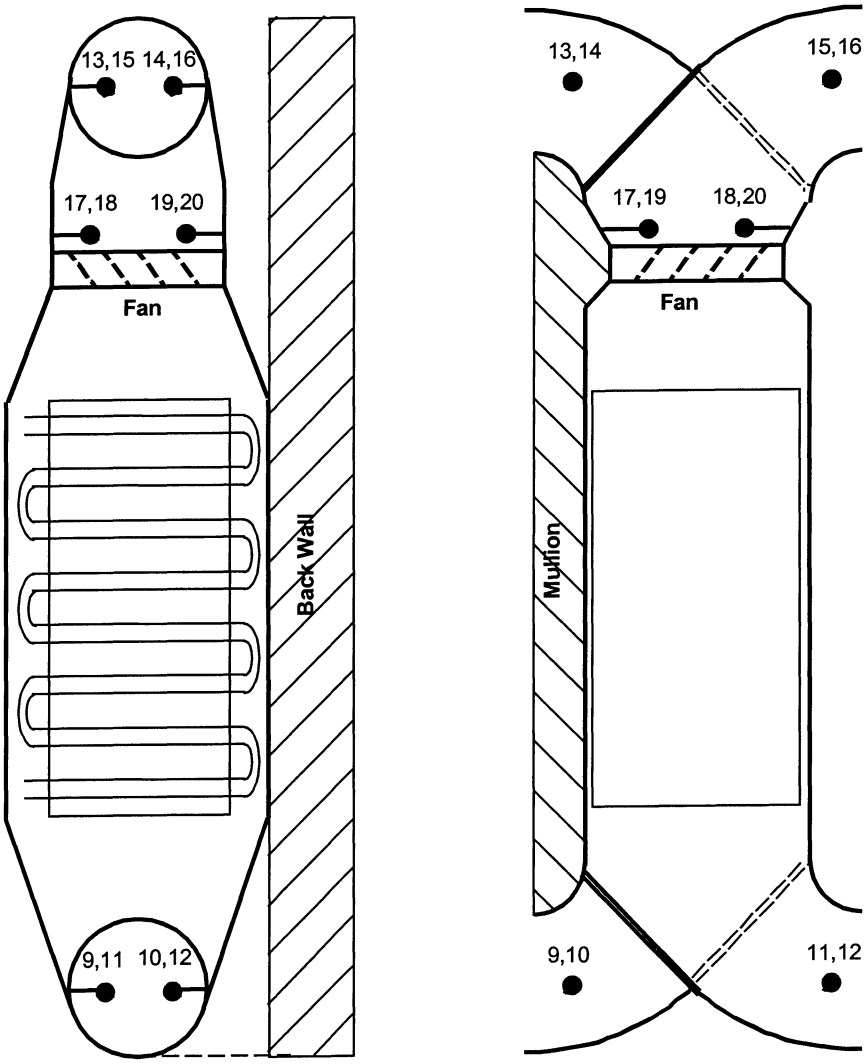

Figure B.1 Air-side evaporator instrumentation

Since the experimental study was primarily concentrating on the evaporator modeling, the new evaporator was instrumented more extensively than before. Two thermocouples were put in each duct leading to or from the evaporator. These thermocouples were mounted roughly 1/3 and 2/3 of the way along the horizontal diameter line of each duct about 0.75" away from the duct opening. These thermocouple locations are numbered 9 through 16 in Figure B.1.

Additionally, four thermocouples were put about 0.5" above the evaporator fan. They were installed in a square pattern as shown in Figure B.1, points 17 through 20. These thermocouples were used to monitor if the air flow temperature was uniform. Also, the average temperature measured by these thermocouples was used to double check the temperature of the air exiting into the compartment that was being cooled, which was also monitored by the thermocouples installed in the air exit ducts (13 and 14 for the freezer or 15 and 16 for the fresh food compartment).

If the temperature of the air inside the duct leading into the compartment other than the one being cooled was lower than the average temperature in that compartment, that could indicate that the valve responsible for switching the flow between the compartments might not be directing the entire flow into the compartment that was supposed to be cooled at this stage in the cycle.

B.2.3 Refrigerant-side instrumentation

Most of the refrigerant-side thermocouples were installed at the same exact locations as previously done by Srichai. New thermocouples were installed at the inlets and exits of the evaporator, captube and compressor.

Additional five surface thermocouples were attached to the evaporator tube bends at the very bottom of each of the three coils and the very top of each of the two coils that were joined together to form the new evaporator prototype. The purpose of these measurement was to determine whether the evaporator dry-out effect for the originally installed coil would be observed in the new evaporator as well.

Just like before, four surface thermocouples were placed around the shell of the new compressor - at the top, bottom, front and back. The average measurement from these thermocouples was used to curve fit the correlation between the compressor shell temperature and the compressor discharge temperature.

The new refrigerant-side instrumentation is shown in Figure B.2.

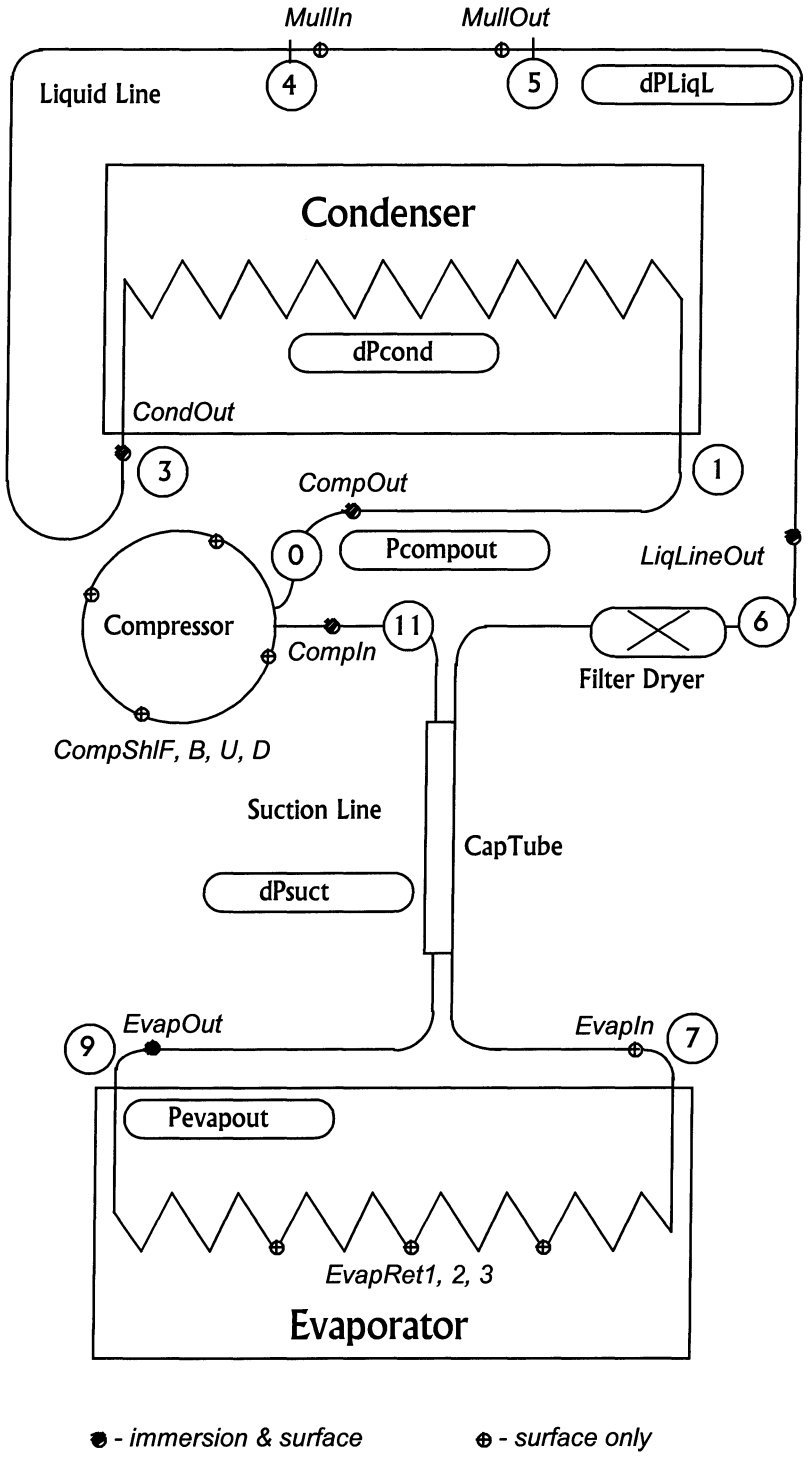

Figure B.2 Refrigerant-side instrumentation

Appendix C

Cabinet Conductance Measurement

The reverse heat leak tests on Amana refrigerator were repeated again to get the real cabinet conductance of the test unit after more than a year of heavy modification and experimental use.

C.1 System setup

During all the reverse heat leakage experiments:

- the compressor was disconnected from its power source;
- both the evaporator and the condenser fans were turned on;
- both mixing-fans (4.025 Watts) in freezer and fresh food cabinets were running during the experiments.

Turning on all the fans was to ensure that the air flow over the condenser and the switching box was generating the same amount of forced convection as it does in all the experiments in which the refrigerator is running. The power was provided directly to the evaporator fan in order to bypass the refrigerator's built-in control system which does not start running the fan until the compressor have been on for a pre-programmed amount of time.

There is certain change on the control volume due to the switching system position between freezing cycle and fridge cycle. So we need to get the UA of both cabinets on both running conditions. We also need to get the UA of the mullion (here means the boundary between freezer and fresh food cabinet, which changes during different kinds of cycles), especially since the mullion is not as a good insulation as before after making two holes on it. When the system is running, we need UA of mullion to know the heat transfer through the mullion.

In order to get an accurate heater power into the cabinets, two variacs were used to supply changeable voltages directly to the heaters. By measuring the voltage and the resistance with a Fluke multi-meter, we can get accurate power inputs during the tests through $W = U^2 / R$. Average temperatures in both cabinets are also recorded. It is not necessary to keep both temperatures same during the test. Two power transducers were also used to get both heater powers simultaneously, it came out that the power meter data were almost same as the data

getting though $W = U^2 / R$, which also proved both power transducers inside the chamber were precise enough for the late tests.

The cabinet temperatures are generally kept about 40-60°F above the chamber temperature when heaters are turned on.

C.2 UA measurement for freezer mode

A schematic drawing of the refrigerator heat transfer during a reverse heat leak test is shown in Figure C.1 for freezer mode.

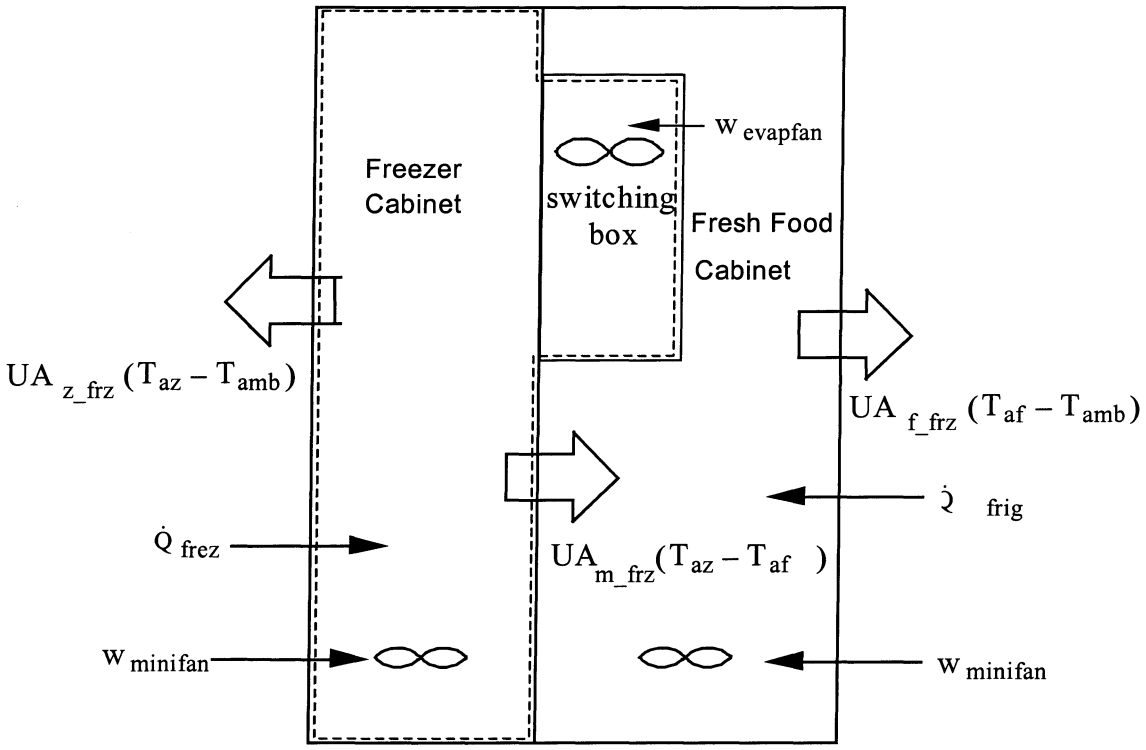

Figure C.1 Control volume for cabinet conductances during freezing cycle

The energy balance equations on freezer cycle are:

$$\dot{Q}_{frez} + w_{evapfan} + w_{minifan} = UA_{z\_frz}(T_{az} - T_{amb}) + UA_{m\_frz}(T_{az} - T_{af}) \qquad (1)$$

$$\dot{Q}_{frig} + w_{minifan} = UA_{f\_frz}(T_{af} - T_{amb}) - UA_{m\_frz}(T_{az} - T_{af}) \qquad (2)$$

The following is test procedure during freezer mode:

First adjust the duct system to freezer mode if it is not in the freezer mode. Then turn on heaters inside both cabinets, adjust both variacs to make sure that both cabinet temperatures are almost 40 °F to 60 °F higher than chamber temperature but not necessary equivalent. Two equations are obtained for each cabinet; Then let $T_{af} = T_{amb}$ by closing heater in the fresh food cabinet and opening that door while keeping the heater in freezer cabinet on and that door closed. One equation are obtained from freezer cabinet energy balance. Therefore, we have three unknowns and three equations. Solve these equations then three UA's are obtained for freezer mode.

C.3 UA measurement for fresh food mode

A schematic drawing of the refrigerator heat transfer during a reverse heat leak test is shown in Figure C.2 for fresh food mode.

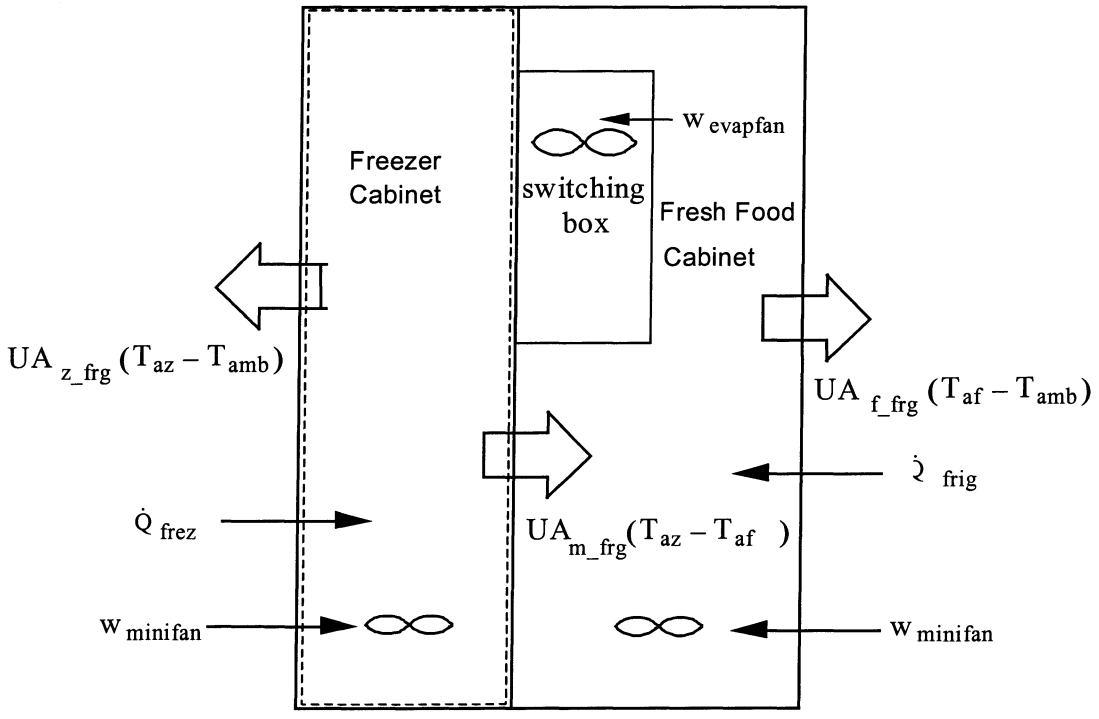

Figure C.2 Control volume for cabinet conductances during fresh food cycle

The energy balance equations on fresh food cycle are:

$$\dot{Q}_{frez} + w_{ninifan} = UA_{z\_frg}(T_{az} - T_{amb}) + UA_{m\_frg}(T_{az} - T_{af}) \quad (3)$$

$$\dot{Q}_{frig} + w_{evapfan} + w_{minifan} = UA_{f\_frg}(T_{az} - T_{amb}) - UA_{m\_frg}(T_{az} - T_{af}) \quad (4)$$

The following is test procedure during fresh food mode:

First adjust the duct system to fresh food mode if it is not in the fresh food mode. Then turn on heaters inside both cabinets, adjust both variacs to make sure that both cabinet temperatures are almost 40 °F to 60 °F higher than chamber temperature but not necessary equivalent. Two equations are obtained for each cabinet; Then let $T_{az} = T_{amb}$ by closing heater in the freezer cabinet and opening that door while keeping the heater in fresh food cabinet on and that door closed. One equation are obtained from fresh food cabinet energy balance. Therefore, we have three unknowns and three equations. Solve these equations then three UA values are obtained for fresh food mode.

C.4 UA results

Table C.1 shows the conductance of our prototype refrigerator.

Condition	chamber temp. setting	Freezer UA (W/F)	Fresh Food UA (W/F)	Mullion UA (W/F)
Freezer mode	65 F (64.9 ~ 65.1 F)	0.9386	0.839	1.064
Fresh Food mode	65 F (64.9 ~ 65.1 F)	0.8568	0.9456	0.7147

Table C.1 Reverse heat leak test results

Appendix D

Capillary Tube Optimization

D.1 Optimization criterion

The goal of system optimization was to seek the highest COP for each mode with a suitable subcooling and superheat under the standard test conditions of 5°F for freezer compartment and 45°F for fresh food compartment respectively with 90°F ambient temperature. The goal was for subcooling to be present, preferably about 5°F in both modes. This allowed for accurate calculation of refrigerant mass flow at the most common operating conditions. The superheat goal for freezer mode optimization was preferably 5°F, and less than 15°F. Finally, the optimum refrigerator charge for both modes had to be the same, which was an additional design constraint.

D.2 Freezer mode optimization

D.2.1 System setup

During freezer mode optimization, the compressor was set at the highest compressor, which is around 3750 rpm, through a special compressor controller supplied by Americold. The Nidec (model TA500DC) DC evaporator fan was operated under a maximum input voltage of 48 VDC, to give a best heat transfer performance over evaporator.

The heater inside the freezer cabinet was turned on to give a controllable heat load for the evaporator. The chamber temperature was set to 90 °F and the freezer temperature at the evaporator inlet was set to 5 °F, which was used to control the heat load of the heater. The heater inside the fresh food was turned off at this time. The fresh food cabinet temperature would reach a stable value which was recorded to calculate the heat leakage into the freezer cabinet.

In order to allow flexibility in using capillary tubes of different diameters and lengths, four capillary tubes were installed in the system which can be selected by three Y-valves. The first and second captubes had internal diameter of 0.028 inches and initial lengths of 10 feet each. The third captube was the same length but measured 0.031 inches in diameter. Finally, the

fourth captube was even thicker, being rated at 0.040 inches ID and longer, having 12 feet in length.

The outlet sections of four parallel captubes were brazed to a the suction line for a length of 5 feet, which is a simple recovery heat exchanger. The adiabatic inlet section of each captube can be "snipped" to provide optimal flow expansion.

Ideally, the captube for freezer mode should be thinner and/or longer compared with fresh food mode. So the first captubes was selected to use during freezer operation, while the third and fourth captubes were meant for fresh food operation. However, before the system can be operating properly in each mode, snipping would be required.

D.2.2 Freezer optimization procedure

At each captube length, first charge 150 grams R-134a (the factory suggested charge). When the system was stable, watch the subcooling and superheat. Then some certain refrigerant was added into system, by 5 to 20 gram each time according to how far the subcooling was from 5°F, until the subcooling approaching to 5°F. If there was too much superheat at that conditon, it indicated that the captube was too long and needed to be cut shorter. To avoid cutting captube too short, 2 inches was cut each time. The COP at each captube length was calculated using the test data at each step, as the maximum COP was approached.

D.2.3 Results

Table D.1 shows the steady-state system performance data from different captube length. Figure D.1 – D.3 shows the change of system performance with refrigerant charge. As we can see, the subcooling decreases while the captube length decreases, but increases while the charge increases; the superheat decreased while the captube length decreases, and also decreases while the charge increases. Therefore, by changing the length of captube and system charge, we can finally reach the optimization point.

Captube Length	Refrigerant Charge	Subcooling (F)	superheat (F)	COP	Cooling Cap. (Watts)	Wevapfan (Watts)	Runtime Fraction
8' 2"	349.4 g	14.17	22.88	1.1792	202.1	10	0.6372085
8' 0"	341.6 g	14.58	16.68	1.22408	219.1	10.6	0.5894227
7' 10"	350.7 g	14.65	12.32	1.22035	221.6	10.6	0.5799266
7' 8"	333.9 g	11.82	18.41	1.18777	208.2	10.6	0.6208202
7' 6"	350 g	11.63	13.37	1.16942	210.3	10.6	0.613718
7' 4"	345.4 g	12.83	5.904	1.20963	227.1	10.6	0.5689692
7' 2"	323.6 g	9.026	18.03	1.15884	208.4	10.6	0.6202134
7' 0"	326.5 g	8.663	13.69	1.11754	196.1	10.34	0.6590026
6' 10"	330.7 g	7.579	8.948	1.08361	188.2	10.6	0.6888518
6' 8"	301.8 g	9.89	28.62	1.03062	171.9	10.6	0.7569608
6' 8"	318.2 g	10.68	20.43	1.10998	192.6	10.6	0.6709362
6' 8"	330 g	11.73	14.07	1.15077	202.2	10.6	0.6383987
6' 8"	341 g	8.847	1.972	1.13864	200	10.6	0.6459999
6' 6"	330 g	9.219	17.01	1.16805	208.7	10.7836	0.6187272
6' 6"	335.6 g	10.41	15.42	1.18404	210.9	10.7836	0.6119585
6' 6"	340.5 g	11.55	14.23	1.1792	211.7	10.7836	0.6101036
6' 6"	345.5 g	12.6	13.38	1.19535	213.9	10.7836	0.60314
6' 6"	349.7 g	13.14	11.17	1.20821	216.6	10.7836	0.596892
6' 6"	352.7 g	13.52	10.43	1.20212	217.3	10.7836	0.593239

Table D.1 Freezer mode performance with various captube length and refrigerant charge

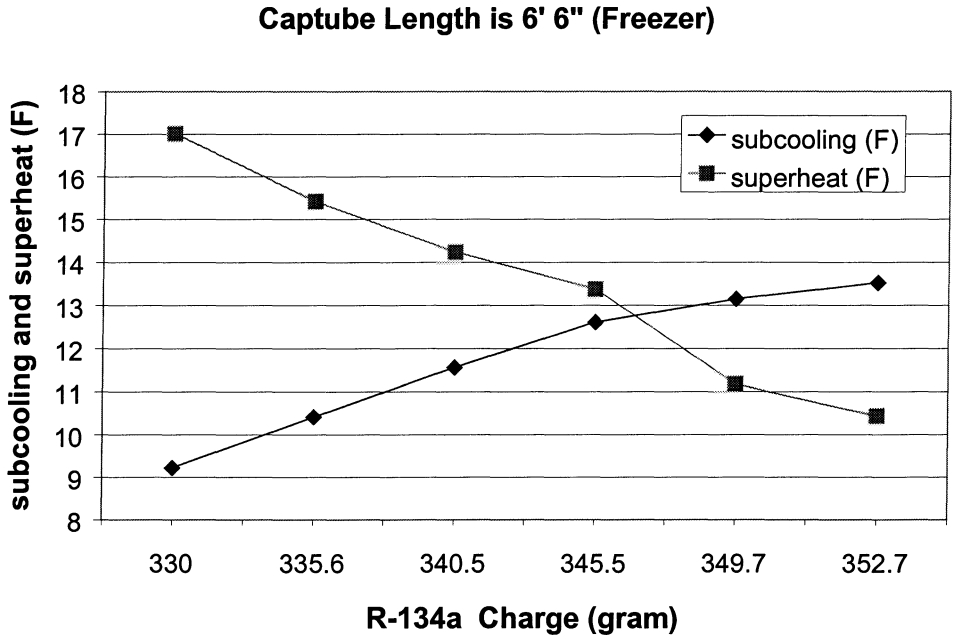

Figure D.1 subcooling and superheat vs. charge

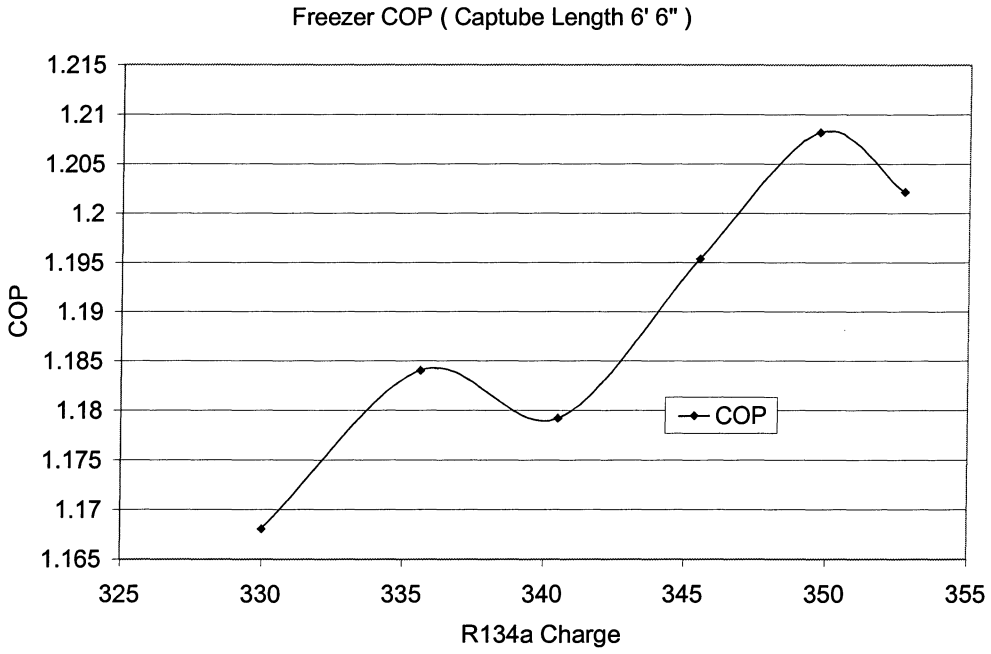

Figure D.2 COP vs. charge

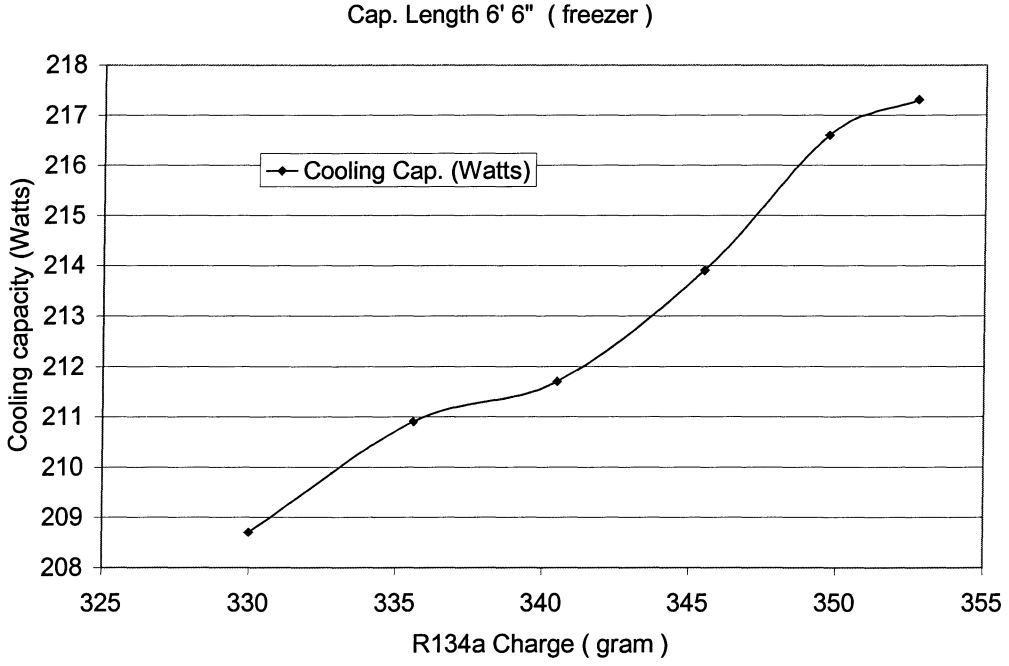

Figure D.3 Cooling capacity vs. charge

At the captube length of 6' 6", the subcooling was about 11 °F and the superheat was about 10 °F , which means we should cut the captube shorter. However, due to the geometric limitation on prototype, we could not cut it more. Finally, the system optimization point for freezer mode was set when the captube length was 6' 6" with a charge of 350 grams. The optimized COP for freezer mode was about D.2. But in the future product of this design, we can get an even better COP with a shorter or larger-diameter captube.

D.3 Fresh food mode optimization

D.3.1 System setup

The optimal system charge was determined during the freezer mode captube and charge optimization. This refrigerant charge (350 grams) was kept the same when we optimized another captube for the fresh food operating mode.

The compressor was set to the lowest speed, which was 1890 rpm, almost half of the higher speed. The DC evaporator fan operated under a maximum input voltage which is 48 VDC, to give a best heat transfer performance over evaporator.

The heater inside the fresh food cabinet was turned on to give a controllable heat load for the evaporator. The chamber temperature was set to 90 °F and the fresh food temperature at the evaporator inlet was set to 45 °F, which was used to control the heat load of the heater. The heater inside the freezer was turned off at this time. The freezer food cabinet temperature would reach a stable value which was recorded to calculate the heat leakage into the fresh food cabinet.

The third captube (originally 10 feet in length and 0.031 inches in diameter) and the fourth captube (originally 12 feet in length and 0.040 inches in diameter) were used in the fresh mode optimization.

D.3.2 Optimization procedure

Since the refrigerant charge was fixed at this time, fresh mode optimization was mainly done by adjusting the length of captube. The objective we sought was to obtain a subcooling of 5 °F and a highest COP.

Optimization was first done on the fourth captube with an original length of 12 feet and diameter of 0.040 inches. It was cut 2" shorter when it was installed. Table D.2 gives the fresh

food mode performance. At this condition, the subcooling was already less than 5 °F. As we know, with a fixed charge, the subcooling decreases when the length of captube decrease. So cutting this captube shorter would make the system away from the optimization point. The real optimized captube length with diameter of 0.040" should be more than 11'10".

Captube Length	11' 10"
Captube Diameter	0.040 "
Refrigerant Charge	350.3 g
subcooling	1.758°F
superheat	15.37°F
Cooling Capacity	275.3 W
COP	1.931

Table D.2 Captube #4 in fresh food mode

The optimization was then conducted on the third captube with a diameter of 0.031". The fresh food mode optimization stopped when we reached 5 °F subcooling. Table D.3 shows the data for fresh food mode optimization procedure. Figure D.4 – D.6 shows the change of system performance with the captube length. The subcooling and superheat decreases while the captube length decreases, which is the same as in freezer mode optimization.

The final optimized captube length for fresh food mode was 7'6" with a diameter of 0.031".

Captube Length	EvapFan Power (W)	Subcooling (°F)	Superheat (°F)	COP	Cooling Cap. (W)	FFC Runtime fraction
9' 7"	10.67	9.686	37.16	1.640998	210.2	0.069454
9' 2"	10.59	8.429	35.83	1.699706	225.1	0.065101
8' 8"	10.56	8.549	34	1.775824	237.9	0.059053
8' 2"	10.51	7.184	30.57	1.810711	248.8	0.058627
7' 10"	10.56	6.334	30.38	1.845481	256.2	0.055473
7' 6"	10.54	5.061	27.62	1.860775	262.9	0.056171

Table D.3 Fresh food mode optimization with a charge of 350 grams

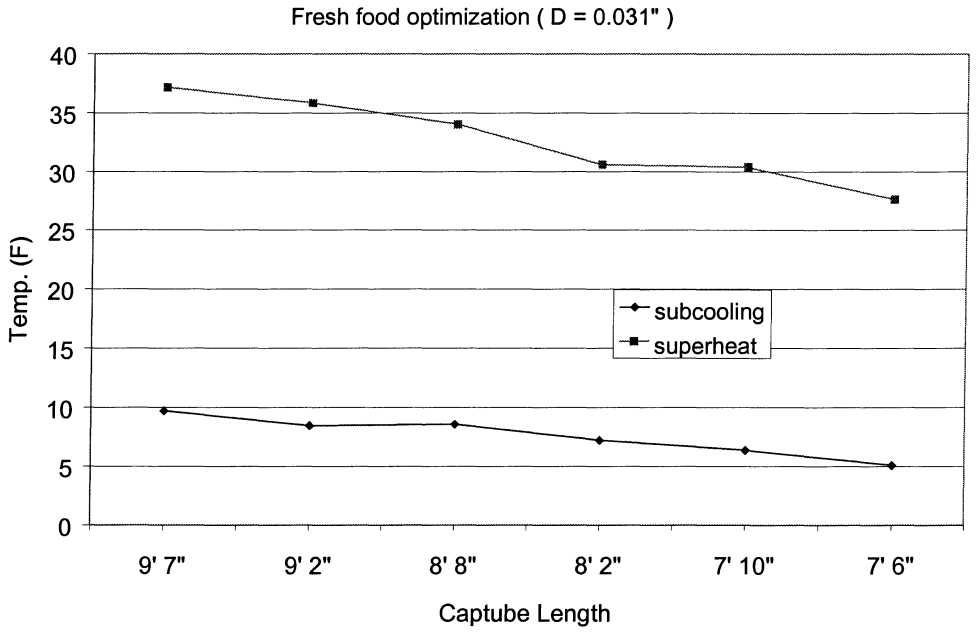

Fig. D.4 subcooling and superheat vs. captube length

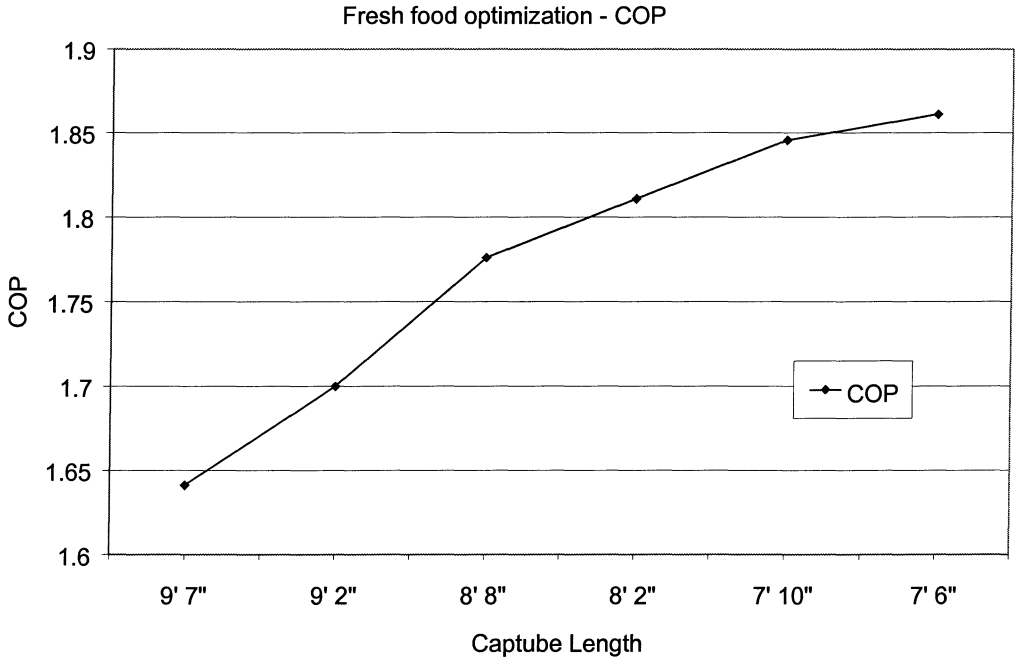

Fig. D.5 COP vs. captube length

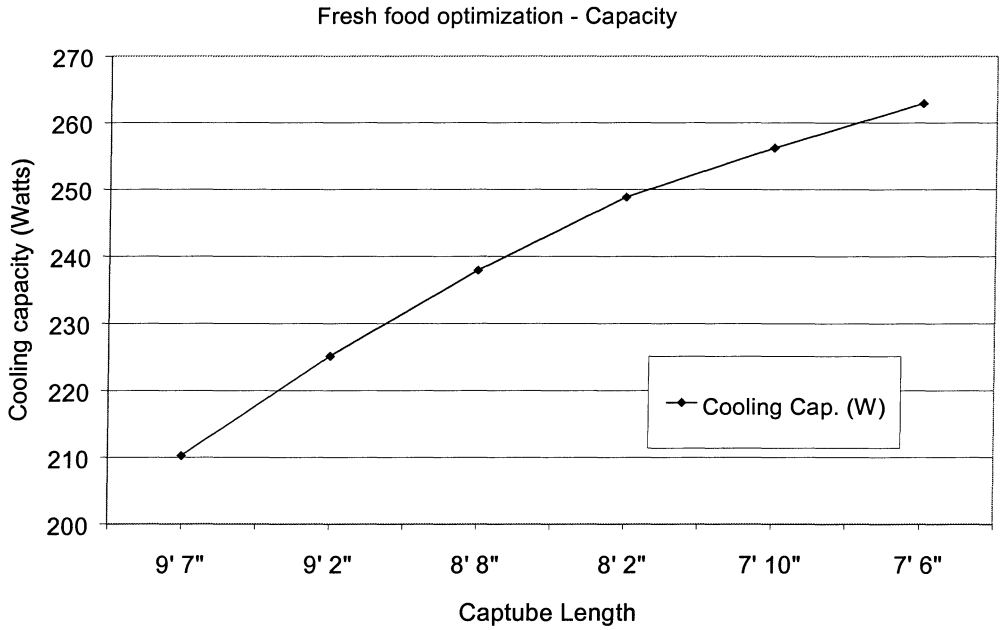

Fig. D.6 Cooling Capacity vs. captube length

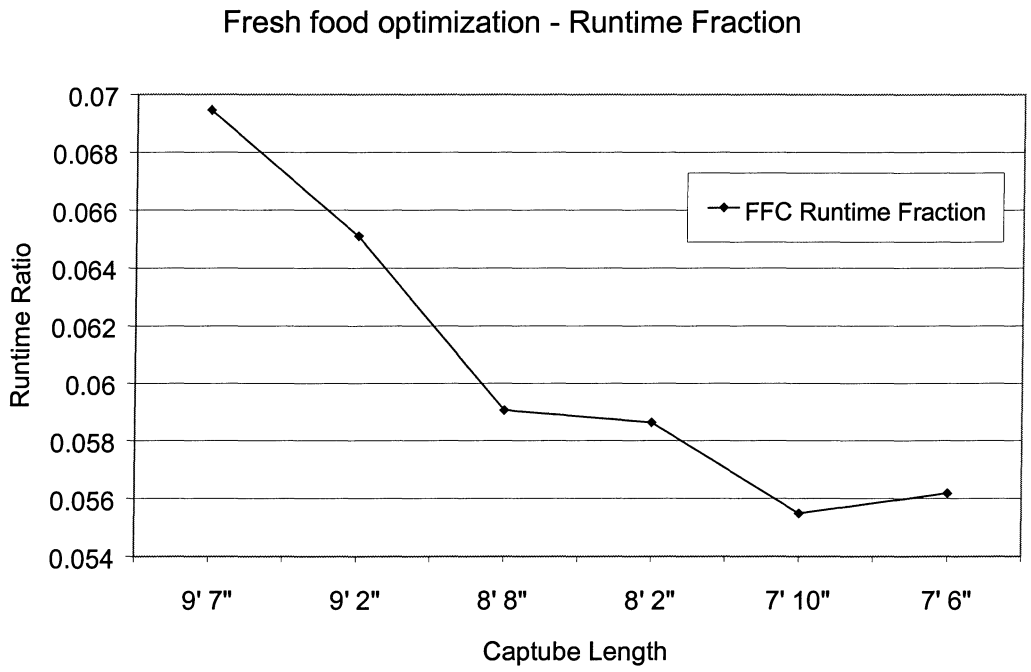

Fig. D.7 Runtime fraction vs. captube length

Kelman (1999) found from his simulation that over 10% more total refrigerant charge is required in fresh food mode than in freezer mode to run the system properly under a turn down

ratio of 2.0. This was also verified by our fresh food optimization experiment. When the subcooling was approaching 5 °F, the superheat was still more than 25 °F, which means we need more refrigerant charge and also shorter captube length if we want the system to run with 5 °F subcooling and 5 °F superheat.

In our test, the charge was kept the same for both freezer mode and fresh food mode. But in the future product of dual-temperature evaporator refrigerator, it might be possible to design an accumulator or a receiver that could release this amount of refrigerant while operating in the fresh food mode and store it during the freezer operation to prevent compressor flooding. Access to this receiver could be controlled by the same solenoid valve that is used to switch the flow between the two captubes. Therefore, higher COP can be obtained for fresh food mode.

Appendix E

Variable Speed Evaporator Fan

The variable speed Nidec fan used here is rated at 150 cfm by manufacturer while operating at its maximum speed when powered by 48 Volts DC. This maximum volumetric flow rate in our situation was only about 50 cfm, due to the pressure drop across our evaporator and duct system. Figure E.1 and E.2 shows the power and volumetric flow rates at both modes.

Fig. E.1 Fan Power vs. Fan Input

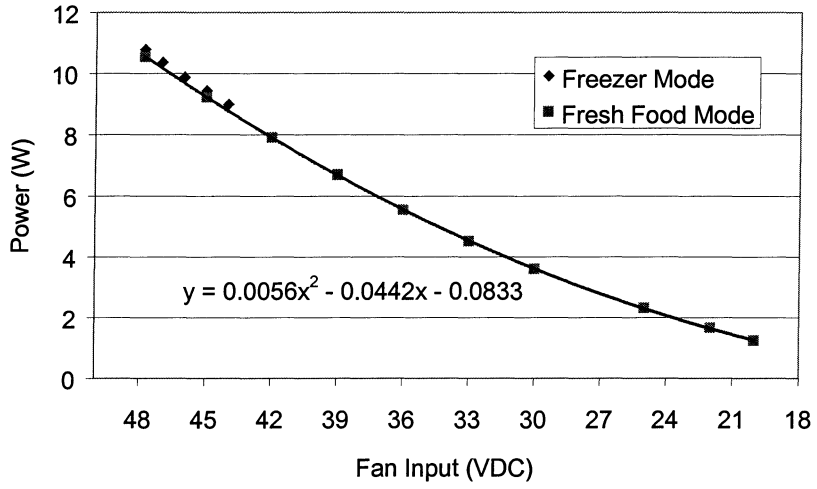

Fig. E.2 Air Flow Rate vs. Fan Input

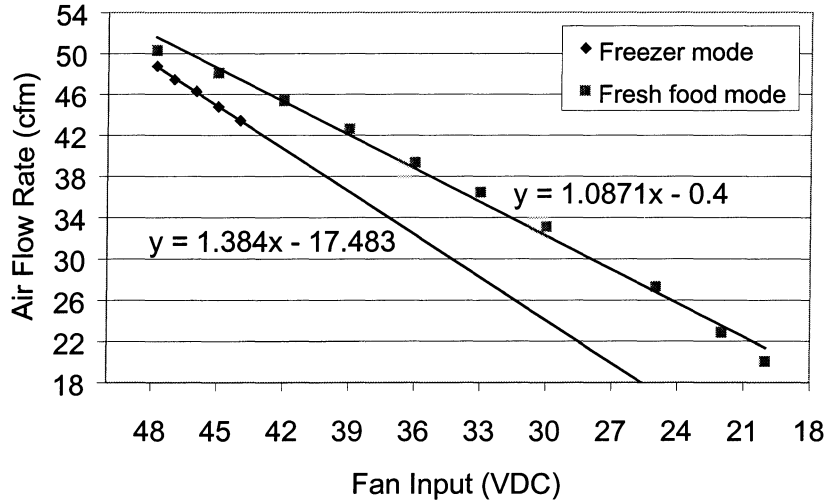

The volumetric flow rate is almost linear with the fan input voltage. The linear function was shown in Fig. E.2. The power shows an almost quadratic function with the fan input voltage. Fig. E.1 and E.2 also showed the power was a little higher and volumetric flow rate was smaller in freezer mode than in fresh food mode. It could be due to the greater frost growth in freezer mode. All tests were conducted with compartment doors closed, in a chamber where the dew point was less than 50 °F, and the only moisture source was leakage into the closed environmental chamber. Nevertheless, small amount of frost accumulation occurred during each test.

Appendix F

Experimental Data Sheets

Table F.1 Freezer mode performance optimization

Comment	# 1 captube with Diameter 0.028" for freezer mode optimization																		
Captube Length	8' 2"	8' 0"	7' 10"	7' 8"	7' 6"	7' 4"	7' 2"	7' 0"	6' 10"	6' 8"	6' 8"	6' 8"	6' 8"	6' 6"	6' 6"	6' 6"	6' 6"	6' 6"	6' 6"
Refrigerant Charge(gram)	349	342	351	334	350	345	323.6	327	331	302	318	330	341	330	335.6	340.5	346	350	353
1:TA: FrezTop	0.1	-0.1	-0.7	-0.1	-1.4	-0.9	-0.5	-2.9	-4.6	1.3	-1.8	-2.8	-3.7	-2.1	-2.2	-2.3	-2.4	-2.6	-2.8
2:TA: FrezBtm	10.3	11.0	10.8	10.7	9.8	11.0	10.2	8.5	8.0	10.2	8.3	7.9	8.4	7.6	7.7	7.8	7.7	7.9	7.7
3:TA: FrezMid	5.3	5.1	5.1	5.2	5.0	5.0	5.2	5.2	5.2	5.3	3.0	2.8	4.6	2.4	2.3	2.3	2.2	2.2	2.1
4:TA: FrezMid_Ctrl											3.1	2.9	4.7	2.4	2.4	2.3	2.3	2.2	2.3
5:TA: FrigTop	44.0	43.6	43.1	43.0	42.7	42.9	42.7	42.1	42.1	50.3	43.4	43.1	43.5	44.8	43.5	43.2	43.1	43.1	42.9
6:TA: FrigBtm	44.4	44.0	43.5	43.4	43.0	43.3	43.1	42.4	42.4	50.7	43.7	43.4	43.7	45.4	44.1	43.8	43.7	43.7	43.5
7:TA: FrigMid	44.7	44.2	43.8	43.7	43.3	43.6	43.3	42.6	42.6	51.0	44.0	43.8	44.1	45.5	44.2	44.0	43.9	43.8	43.6
8:TA: FrigMid_Ctrl																			
9:TA: FrmFrezFront	7.3	7.6	7.4	7.4	6.4	7.3	6.9	5.2	4.9	7.0									
10:TA: FrmFrezBack	8.2	8.3	8.4	8.2	7.6	8.6	8.0	6.5	5.9	7.7	5.6	5.7	6.1	5.4	5.5	5.4	5.3	5.4	5.3
11:TA: FrmFrigFront	43.4	43.0	42.4	42.2	41.8	42.2	41.9	41.2	41.2	49.3	42.2	42.1	42.4	43.9	42.7	42.5	42.4	42.2	42.0
12:TA: FrmFrigBack	42.9	42.6	41.9	41.7	41.4	41.7	41.4	40.7	40.7	48.9	41.8	41.6	41.9	43.3	42.1	41.9	41.8	41.7	41.5
13:TA:ToFrezFront	-3.0	-3.7	-4.6	-3.5	-5.5	-4.7	-4.2	-7.1	-9.6	-1.0	-5.0	-6.2	-8.1	-4.8	-5.1	-5.2	-5.5	-5.7	-6.2
14:TA: ToFrezBack	-3.2	-3.8	-4.7	-3.7	-5.7	-4.8	-4.4	-7.2	-9.6	-1.1	-5.1	-6.4	-8.3	-5.0	-5.3	-5.4	-5.7	-5.8	-6.3
15:TA: ToFrigFront	42.1	42.0	41.5	41.5	41.1	41.4	40.9	40.4	40.5	48.4	41.4	41.4	42.0	42.7	41.6	41.6	41.4	41.5	41.1
16:TA: ToFrigBack	38.9	38.5	38.1	37.5	37.8	37.6	37.7	37.5	37.7	45.0	37.7	37.8	38.7	39.4	38.2	38.2	37.9	37.9	37.7
17:TA: EvapFanA	-3.0	-3.6	-4.6	-3.6	-5.3	-4.9	-3.9	-7.1	-10.1	-0.7	-4.8	-6.4	-8.4	-5.0	-5.2	-5.4	-5.6	-5.9	-6.3
18:TA: EvapFanB	-3.5	-4.2	-4.8	-4.1	-5.5	-5.3	-4.2	-6.9	-10.1	-1.8	-5.3	-6.5	-8.4	-6.3	-6.4	-6.4	-6.5	-6.6	-6.9
19:TA: EvapFanC	-3.9	-4.1	-5.0	-4.2	-5.8	-5.0	-4.8	-7.5	-10.2	-2.2	-5.6	-6.8	-8.7	-6.1	-6.1	-6.1	-6.2	-6.3	-6.6
20:TA: EvapFanD	-1.9	-2.7	-4.4	-2.6	-5.1	-4.7	-3.1	-7.0	-10.2	1.2	-3.6	-6.0	-8.7	-4.4	-4.7	-4.9	-5.2	-5.6	-6.0
21:TA: GrilleIn_CondIn	89.4	89.9	89.4	89.9	89.6	90.1	89.7	89.6	89.7	89.4	89.4	89.5	89.9	89.5	89.5	89.6	89.5	89.9	89.5
22:TA: CondFanOut	93.5	94.2	93.7	94.1	93.9	94.7	94.2	93.9	93.3	93.5	94.3	95.1	93.3	93.9	94.1	94.0	93.9	94.4	94.2
23:TA: CompIn	100.4	101.6	101.1	100.8	101.3	102.5	101.0	100.4	99.8	99.5	100.2	100.8	100.5	100.7	100.7	101.0	101.0	101.4	101.2
24:TA: Chamber	90.1	90.6	90.0	90.4	90.2	90.9	90.4	90.1	90.0	89.7	89.8	90.0	90.0	90.1	90.1	90.3	90.2	90.5	90.2
25:TR: CompIn	85.9	86.1	86.0	87.4	87.2	87.9	90.1	89.2	88.9	87.2	86.4	85.9	80.1	85.9	85.4	85.0	84.5	84.3	83.9

26:TS: CompIn	92.6	92.9	94.6	95.5	95.5	96.3	95.3	94.8	94.4	92.9	92.3	92.0	87.8	91.9	91.5	91.3	90.9	91.0	90.5
27:TR: CompOut	182.7	185.4	185.3	182.9	185.0	188.0	185.4	183.2	181.4	179.2	181.4	182.3	181.0	184.0	183.4	183.5	183.6	183.9	184.4
28:TS: CompOut	125.3	127.5	127.1	125.9	127.0	129.1	127.1	125.8	124.8	123.8	125.2	125.8	125.5	126.1	126.1	126.5	126.5	126.9	126.8
29:TR: CondOut	104.7	106.7	106.6	105.7	105.7	108.1	105.3	104.3	103.8	102.6	103.8	104.9	104.4	105.0	105.3	105.7	105.9	106.5	106.3
30:TS: CondOut	104.8	106.8	106.7	105.7	105.8	108.0	105.4	104.4	103.9	102.8	103.9	105.0	104.5	105.0	105.3	105.7	105.9	106.5	106.3
31:TS: MullionIn	104.7	106.8	106.7	105.8	105.9	108.1	105.4	104.5	103.9	102.7	103.8	104.9	104.4	105.0	105.3	105.8	105.9	106.5	106.3
32:TS: MullionOut	103.7	105.8	105.7	105.0	105.1	107.1	104.6	103.7	103.2	100.8	101.7	102.4	102.6	104.2	104.5	104.8	104.8	105.2	104.3
33:TR: LiqLineOut	91.5	93.6	93.6	95.1	95.7	97.0	97.9	97.1	97.4	92.2	92.5	92.6	95.0	95.1	94.2	93.5	92.7	92.8	92.3
34:TS: LiqLineOut	92.1	94.1	94.2	95.5	96.0	97.3	97.9	97.1	97.4	92.8	93.1	93.3	95.4	95.5	94.7	94.1	93.4	93.5	93.0
35:TS: EvapIn	-14.1	-11.1	-10.9	-11.9	-12.2	-9.4	-12.0	-14.1	-16.0	-15.8	-14.1	-13.3	-14.1	-11.6	-11.3	-11.0	-11.0	-10.6	-10.9
36:TS: EvapBendIn	-11.1	-8.3	-8.1	-9.0	-9.3	-6.7	-9.1	-11.4	-13.2	-12.1	-11.1	-10.4	-10.9	-8.9	-8.6	-8.4	-8.3	-8.1	-8.3
45:TS: EvapBendIn_Mid	-13.4	-10.6	-10.5	-11.3	-12.2	-8.9	-11.7	-13.7	-15.6	-14.8	-13.6	-12.6	-13.2	-11.2	-10.9	-10.7	-10.6	-10.2	-10.6
37:TS: EvapBendMid	-10.1	-8.4	-7.7	-8.5	-9.0	-5.7	-8.3	-11.3	-13.3	-2.4	-10.1	-9.9	-10.5	-9.3	-9.1	-9.0	-9.0	-8.7	-9.0
46:TS: EvapBendMid_Out	-14.3	-11.8	-11.7	-12.6	-13.4	-10.2	-12.9	-15.0	-16.7	-5.3	-14.7	-13.8	-14.3	-12.3	-12.0	-11.8	-11.8	-11.4	-11.8
38:TS: EvapBendOut	5.0	1.4	-10.5	3.4	-11.7	-9.4	2.2	-13.4	-15.9	6.6	2.7	-10.9	-13.8	1.6	-0.1	-3.1	-6.4	-10.4	-10.9
39:TR: EvapOut	2.2	-0.5	-4.0	0.5	-4.4	-8.7	-0.2	-6.2	-11.9	5.6	0.0	-4.7	-16.0	-0.8	-1.9	-2.7	-3.3	-4.9	-5.9
40:TS: EvapOut	1.9	-0.5	-3.8	0.3	-4.2	-8.6	-0.3			5.0	-0.3	-4.5	-16.1	-1.0	-1.9	-2.6	-3.3	-4.7	-5.7
41:TS: CompShiTop	152.0	154.1	153.9	152.8	154.0	156.1	153.9	152.4	151.6	150.1	151.4	152.2	150.8	152.2	151.9	152.1	152.1	152.7	152.5
42:TS: CompShiBtm	176.2	177.3	177.4	176.5	178.0	179.6	178.2	177.0	176.0	174.9	176.1	176.7	174.8	175.4	175.2	175.5	175.5	175.9	176.1
43:TS: CompShiUpStrm	160.1	162.0	161.9	161.0	162.0	163.8			159.5	158.3	159.6	160.4							
44:TS: CompShiDnStrm	147.8	149.2	149.3	148.1	148.9	150.2	148.6	147.1	147.2	145.2	146.2	147.0	147.4	147.5	147.4	147.7	147.6	148.0	147.8
Power1:InWallLeft	5.6	5.5	5.6	5.4	5.6	5.6	5.7	5.6	5.7	5.5	5.5	5.5	5.3	5.6	5.4	5.4	5.4	5.4	5.5
Power2:InWallRight	147.3	154.2	156.7	150.3	154.6	162.7	154.4	150.2	147.6	140.4	147.8	150.4	150.4	153.1	152.8	154.2	153.7	154.2	155.5
Power3:Frez	70.9	87.0	90.5	77.1	79.3	95.2	77.5	66.5	58.5	34.4	57.6	66.2	64.6	70.5	74.0	74.9	77.1	79.4	80.4
Power4:FFC	0.0	0.0	0.0	0.0	0.0	0.0	0.0	0.0	0.0	0.0	0.0	0.0	0.0	0.0	0.0	0.0	0.0	0.0	0.0
Power5:OutWall	140.4	147.3	149.5	143.6	147.8	155.5	147.3	143.4	141.1	134.2	141.0	143.6	143.4	146.1	145.4	147.3	146.4	147.4	148.6
1:Press:CondOut	152.6	158.4	158.5	155.6	156.5	162.2	155.4	152.7	151.0	149.4	153.0	155.8	154.9	154.1	154.8	155.9	156.4	157.7	157.5
2:D_P:Cond	4.20	5.14	5.60	5.13	5.41	6.45	5.41	5.00	4.67	3.87	4.67	5.07	5.46	5.57	5.56	5.58	5.54	5.63	5.68
3:D_P:LiqLine	1.46	1.47	1.37	1.46	1.50	1.36	1.26	1.28	1.21	1.27	1.30	1.35	1.22	1.41	1.50	1.45	1.32	1.27	1.16
4:Press:EvapOut	12.70	13.92	14.22	13.66	13.71	14.88	13.54	12.97	12.67	11.95	12.80	13.38	13.63	13.69	13.88	14.02	14.09	14.31	14.22

5:D_P:SucLine	0.68	0.68	0.79	0.69	0.77	0.75	0.73	0.66	0.71	0.59	0.66	0.68	0.62	0.73	0.73	0.72	0.74	0.74	0.76
6:Press:Chamber	14.75	14.69	14.72	14.71	14.72	14.72	14.77	14.82	14.80	14.64	14.60	14.58	14.53	14.72	14.71	14.71	14.70	14.68	14.63
subcooling	14.2	14.6	14.7	11.8	11.6	12.8	9.026	8.66	7.58	9.89	10.7	11.7	8.85	9.22	10.41	11.55	12.6	13.1	13.5
superheat	22.9	16.7	12.3	18.4	13.4	5.9	18.03	13.7	8.95	28.6	20.4	14.1	1.97	17	15.42	14.23	13.4	11.2	10.4
COP	1.179	1.224	1.220	1.188	1.169	1.210	1.159	1.118	1.084	1.031	1.110	1.151	1.139	1.168	1.184	1.179	1.195	1.208	1.202
Cooling Cap. (W)	202	219	222	208	210	227	208.4	196	188	172	193	202	200	209	210.9	211.7	214	217	217
Wevapfan (W)	10	10.6	10.6	10.6	10.6	10.6	10.6	10.3	10.6	10.6	10.6	10.6	10.6	10.8	10.78	10.78	10.8	10.8	10.8
FRZ Runtime Fraction	0.637	0.589	0.580	0.621	0.614	0.569	0.620	0.659	0.689	0.757	0.671	0.638	0.646	0.619	0.612	0.610	0.603	0.597	0.593
Day	3	4	6	10	11	14	15	17	19	26	26	27	28	8	8	8	8	8	8
Month	6	6	6	6	6	6	6	6	6	6	6	6	6	7	7	7	7	7	7
Year	1999	1999	1999	1999	1999	1999	1999	1999	1999	1999	1999	1999	1999	1999	1999	1999	1999	1999	1999

Table F.2 Fresh food mode performance optimization

Comment	# 3 captube, Diameter = 0.031" for fresh food optimization					
Captube Length	9' 7"	9' 2"	8' 8"	8' 2"	7' 10"	7' 6"
Refrigerant Charge	350.3 g	350 g	350 g	350.6 g	350 g	350 g
1:TA: FrezTop	61.8	64.0	62.3	62.6	62.9	63.5
2:TA: FrezBtm	62.7	65.1	63.0	63.4	63.7	64.3
3:TA: FrezMid	62.1	64.4	62.5	62.7	63.0	63.5
4:TA: FrezMid_Ctrl						
5:TA: FrigTop	36.2	36.4	35.8	34.9	35.6	34.7
6:TA: FrigBtm	43.9	43.6	43.6	42.9	44.0	43.2
7:TA: FrigMid	46.5	46.5	46.9	46.4	47.7	46.9
8:TA: FrigMid_Ctrl	46.3	46.2	46.6	46.1	47.4	46.6
9:TA: FrmFrezFront	58.7	60.7	59.1	59.1	59.4	59.6
10:TA: FrmFrezBack	57.8	59.7	58.1	58.1	58.5	58.7
11:TA: FrmFrigFront						
12:TA: FrmFrigBack	45.6	45.6	45.8	45.4	46.6	45.8
13:TA:ToFrezFront	51.9	52.9	51.3	51.5	51.6	51.8
14:TA: ToFrezBack	44.5	45.7	45.0	44.7	45.4	45.1
15:TA: ToFrigFront	32.9	32.8	32.1	31.6	31.9	31.1
16:TA: ToFrigBack	32.9	33.1	32.6	31.7	32.3	31.1
17:TA: EvapFanA	33.3	34.7	34.1	32.8	33.6	32.3
18:TA: EvapFanB	31.7	30.6	30.1	29.1	29.9	29.0
19:TA: EvapFanC	30.5	29.9	29.4	28.2	29.0	27.8
20:TA: EvapFanD	35.6	37.1	36.2	34.7	35.2	33.9
21:TA: GrilleIn_CondIn	89.2	89.3	88.6	89.2	88.8	89.4
22:TA: CondFanOut	92.8	93.1	92.6	93.3	92.9	93.7
23:TA: CompIn	99.4	100.1	99.8	100.8	100.7	101.6
24:TA: Chamber	89.9	90.0	89.4	90.0	89.6	90.2
25:TR: CompIn	88.7	90.0	89.7	91.1	91.5	92.4
26:TS: CompIn	93.3	94.3	94.0	95.3	95.4	96.3
27:TR: CompOut	161.8	163.8	163.9	166.1	166.3	167.8
28:TS: CompOut	117.8	119.0	118.9	120.4	120.4	121.5
29:TR: CondOut	106.3	107.4	107.5	109.0	108.9	109.8
30:TS: CondOut	106.2	107.3	107.4	108.9	108.7	109.7
31:TS: MullionIn	106.4	107.4	107.5	109.0	108.9	109.9
32:TS: MullionOut	105.3	106.6	106.8	108.3	108.1	109.1
33:TR: LiqLineOut	96.0	98.4	98.3	101.2	102.0	104.3
34:TS: LiqLineOut	96.1	98.2	98.2	100.9	101.5	103.8
35:TS: EvapIn	11.6	14.4	15.7	17.7	18.8	20.2
36:TS: EvapBendIn	15.5	18.4	19.4	20.9	21.7	22.6
45:TS: EvapBendIn_Mid	11.8	14.5	15.8	17.6	18.6	19.8
37:TS: EvapBendMid	40.3	42.5	40.3	25.6	23.2	23.4
46:TS: EvapBendMid_Out	27.8	35.6	33.5	30.1	29.7	26.4
38:TS: EvapBendOut	44.1	44.8	44.7	43.8	44.8	43.8
39:TR: EvapOut	44.3	45.8	45.3	44.2	44.9	43.8
40:TS: EvapOut	46.0	47.4	46.8	45.7	46.4	45.3

41:TS: CompShiTop	135.5	137.1	137.0	138.8	138.7	140.1
42:TS: CompShiBtm	147.8	149.3	148.6	150.0	149.7	150.7
43:TS: CompShiUpStrm						
44:TS: CompShiDnStrm	130.9	132.3	132.0	133.6	133.5	134.8
Power1:InWallLeft	5.55	5.56	5.58	5.42	5.52	5.46
Power2:InWallRight	105.37	110.06	111.88	115.67	117.02	119.62
Power3:Frez	0.00	0.00	-0.01	0.00	-0.01	-0.01
Power4:FFC	140.18	153.28	167.92	177.05	186.24	190.49
Power5:OutWall	101.74	105.79	107.15	111.09	111.98	114.85
1:Press:CondOut	157.44	160.88	161.42	165.34	165.68	168.80
2:D_P:Cond	4.64	5.69	6.22	6.84	7.24	7.79
3:D_P:LiqLine	1.44	1.28	1.42	1.28	1.29	1.00
4:Press:EvapOut	25.01	26.62	27.46	28.86	29.48	30.52
5:D_P:SucLine	0.36	0.40	0.40	0.42	0.43	0.48
6:Press:Chamber	14.78	14.76	14.76	14.74	14.73	14.71
EvapFan Power (W)	10.67	10.59	10.56	10.51	10.56	10.54
subcooling	9.686	8.429	8.549	7.184	6.334	5.061
superheat	37.16	35.83	34	30.57	30.38	27.62
COP	1.641	1.700	1.776	1.811	1.845	1.861
Cooling Cap. (W)	210.2	225.1	237.9	248.8	256.2	262.9
FFC Runtime Fraction	0.0695	0.0651	0.0591	0.0586	0.0555	0.0562
Day	11	11	12	12	13	13
Month	7	7	7	7	7	7
Year	1999	1999	1999	1999	1999	1999

Table F.3 Freezer system performance with variable fan speeds

	Freezer mode performance with variable speed evaporator fan					
	# 1 captube, Diameter = 0.028", L = 6' 6", Charge is 350 g					
EvapFan Volt	47.8	47	46	45	44	43
EvapFan Current	0.2256	0.2204	0.2146	0.2095	0.2041	0.1975
EvapFan Power	10.78	10.36	9.87	9.43	8.98	4.52
1:TA: FrezTop	-2.8	-2.9	-3.0	-3.1	-3.1	-3.2
2:TA: FrezBtm	7.7	7.7	7.8	8.2	8.0	8.4
3:TA: FrezMid	2.1	2.3	2.5	3.1	3.1	3.5
4:TA: FrezMid_Ctrl	2.3	2.5	2.7	3.2	3.2	3.6
5:TA: FrigTop	42.9	43.0	43.0	43.2	44.4	43.4
6:TA: FrigBtm	43.5	43.5	43.5	43.7	44.8	43.8
7:TA: FrigMid	43.6	43.7	43.7	43.8	45.0	44.0
8:TA: FrigMid_Ctrl						
9:TA: FrmFrezFront						
10:TA: FrmFrezBack	5.3	5.5	5.7	6.3	6.0	6.3
11:TA: FrmFrigFront	42.0	42.0	42.0	42.2	43.4	42.4
12:TA: FrmFrigBack	41.5	41.5	41.5	41.7	42.9	41.8
13:TA:ToFrezFront	-6.2	-6.4	-6.6	-6.7	-6.8	-6.9
14:TA: ToFrezBack	-6.3	-6.6	-6.7	-6.9	-7.0	-7.1
15:TA: ToFrigFront	41.1	41.1	41.1	41.6	42.8	41.8
16:TA: ToFrigBack	37.7	37.8	38.0	38.4	39.9	38.7
17:TA: EvapFanA	-6.3	-6.5	-6.7	-7.0	-7.0	-7.3
18:TA: EvapFanB	-6.9	-7.0	-7.2	-7.4	-7.3	-7.6
19:TA: EvapFanC	-6.6	-6.8	-7.0	-7.4	-7.4	-7.5
20:TA: EvapFanD	-6.0	-6.2	-6.4	-6.9	-7.2	-7.3
21:TA: GrilleIn_CondIn	89.5	89.4	89.3	89.1	89.5	89.2
22:TA: CondFanOut	94.2	94.1	93.8	93.5	93.9	93.6
23:TA: CompIn	101.2	101.0	101.0	100.6	100.8	100.7
24:TA: Chamber	90.2	90.1	90.0	89.8	90.2	89.9
25:TR: CompIn	83.9	83.7	83.6	83.3	78.5	79.8
26:TS: CompIn	90.5	90.3	90.3	90.0	86.3	87.4
27:TR: CompOut	184.4	184.4	184.4	183.2	182.3	182.8
28:TS: CompOut	126.8	126.6	126.6	126.1	126.1	126.2
29:TR: CondOut	106.3	106.1	106.0	105.7	105.7	105.5
30:TS: CondOut	106.3	106.0	106.0	105.7	105.7	105.6
31:TS: MullionIn	106.3	106.1	106.0	105.7	105.7	105.6
32:TS: MullionOut	104.3	104.2	104.3	104.3	104.9	104.8
33:TR: LiqLineOut	92.3	92.2	92.3	92.2	99.2	97.3
34:TS: LiqLineOut	93.0	92.9	92.9	92.8	99.1	97.4
35:TS: EvapIn	-10.9	-11.0	-11.1	-11.3	-11.1	-11.1
36:TS: EvapBendIn	-8.3	-8.4	-8.5	-8.7	-8.4	-8.4
45:TS: EvapBendIn_Mid	-10.6	-10.9	-11.0	-11.0	-10.7	-10.7
37:TS: EvapBendMid	-9.0	-9.1	-9.1	-9.3	-9.0	-9.0
46:TS: EvapBendMid_Out	-11.8	-12.1	-12.2	-12.1	-11.7	-11.7

38:TS: EvapBendOut	-10.9	-11.0	-11.2	-11.5	-11.2	-11.3
39:TR: EvapOut	-5.9	-6.3	-6.9	-8.6	-13.4	-13.4
40:TS: EvapOut	-5.7	-6.1	-6.6	-8.2	-13.5	-13.6
41:TS: CompShiTop	152.5	152.2	152.1	151.7	151.1	151.6
42:TS: CompShiBtm	176.1	176.0	176.0	174.8	174.0	174.3
43:TS: CompShiUpStrm				159.7	159.3	159.6
44:TS: CompShiDnStrm	147.8	147.6	147.5	147.0	146.4	146.8
Power1:InWallLeft	5.48	5.50	5.52	5.43	5.35	5.38
Power2:InWallRight	155.53	157.05	156.44	154.11	156.62	155.73
Power3:Frez	80.44	81.44	82.93	82.37	76.89	82.26
Power4:FFC	0.00	0.00	0.00	0.00	0.00	0.00
Power5:OutWall	148.61	149.58	148.84	147.39	147.95	148.44
1:Press:CondOut	157.54	157.15	156.99	155.96	156.85	156.25
2:D_P:Cond	5.68	5.70	5.74	5.61	6.54	6.35
3:D_P:LiqLine	1.16	1.23	1.22	1.29	1.25	1.34
4:Press:EvapOut	14.22	14.14	14.14	14.10	14.56	14.48
5:D_P:SucLine	0.76	0.73	0.77	0.72	0.66	0.67
6:Press:Chamber	14.63	14.64	14.64	14.64	14.63	14.63
Air Vol. Flow rate (cfm)	48.74	47.42	46.28	44.78	43.41	42.27
subcooling (F)	13.52	13.29	13.17	12.99	5.974	7.614
superheat (F)	10.43	10.22	9.611	8.062	2.022	2.218
COP	1.202	1.199	1.215	1.228	1.192	1.276
Cooling Cap. (W)	217.3	217.7	218.6	217	212.8	215.9
FFC Runtime Ratio	0.593	0.590	0.586	0.588	0.601	0.578
Day	8	8	8.28	9	9	9
Month	7	7	7	7	7	7
Year	1999	1999	1999	1999	1999	1999

Table F.4 Fresh food system performance with variable fan speeds

	Fresh food mode performance with variable speed evaporator fan									
	# 3 captube, Diameter = 0.031", L = 7' 6", Charge is 350 g									
EvapFan Volt	47.8	45	42	39	36	33	30	25	22	20
EvapFan Current	0.2205	0.205	0.1882	0.1716	0.1541	0.1369	0.1198	0.0926	0.0758	0.0621
EvapFan Power	10.54	9.225	7.9044	6.6924	5.5476	4.5177	3.594	2.315	1.6676	1.242
1:TA: FrezTop	63.5	63.3	63.3	63.1	63.0	62.7	63.2	63.5	63.7	63.3
2:TA: FrezBtm	64.3	64.0	64.1	63.9	63.8	63.6	64.1	64.5	65.0	64.8
3:TA: FrezMid	63.5	63.3	63.3	63.2	63.1	62.9	63.5	64.0	64.4	64.1
4:TA: FrezMid_Ctrl										
5:TA: FrigTop	34.7	34.4	33.8	33.0	31.5	30.5	31.9	35.6	44.2	46.7
6:TA: FrigBtm	43.2	43.4	43.5	43.5	43.0	43.1	44.7	45.0	45.5	44.9
7:TA: FrigMid	46.9	47.2	47.1	47.1	46.4	46.3	47.8	49.3	49.8	48.9
8:TA: FrigMid_Ctrl	46.6	46.9	46.8	46.8	46.1	45.9	47.6	49.1	49.7	48.7
9:TA: FrmFrezFront	59.6	59.5	59.5	59.6	59.4	59.2	59.6	60.1	60.7	60.5
10:TA: FrmFrezBack	58.7	58.6	58.6	58.7	58.6	58.4	58.8	59.4	60.0	59.8
11:TA: FrmFrigFront										
12:TA: FrmFrigBack	45.8	46.0	45.9	45.8	45.0	44.4	45.3	45.1	45.9	45.5
13:TA:ToFrezFront	51.8	51.6	51.6	51.9	52.3	52.4	52.3	51.8	50.8	50.6
14:TA: ToFrezBack	45.1	45.1	44.9	44.7	43.9	43.2	42.9	42.8	43.3	46.2
15:TA: ToFrigFront	31.1	30.4	29.6	28.4	26.7	24.9	24.3	20.9	18.4	16.9
16:TA: ToFrigBack	31.1	30.7	29.8	28.7	26.7	24.9	24.1	21.1	18.7	17.0
17:TA: EvapFanA	32.3	31.9	30.9	29.4	26.8	24.7	24.2	20.5	17.7	15.6
18:TA: EvapFanB	29.0	28.6	27.8	27.0	25.3	23.7	23.3	20.2	17.7	15.6
19:TA: EvapFanC	27.8	27.4	26.6	26.2	24.9	23.3	22.7	19.8	17.4	15.3
20:TA: EvapFanD	33.9	33.3	32.4	31.0	28.2	25.7	25.7	21.3	17.9	15.6
21:TA: GrilleIn_CondIn	89.4	89.2	89.0	88.8	89.0	89.3	88.7	88.8	88.9	89.0
22:TA: CondFanOut	93.7	93.4	93.2	92.9	93.1	93.4	92.8	92.8	92.8	92.8
23:TA: CompIn	101.6	101.3	101.0	100.7	100.8	101.0	100.3	100.2	100.0	99.6
24:TA: Chamber	90.2	90.0	89.8	89.7	89.9	90.1	89.6	89.8	89.8	89.9
25:TR: CompIn	92.4	92.2	92.0	91.9	91.8	91.6	90.7	89.9	88.6	86.7
26:TS: CompIn	96.3	96.0	95.8	95.7	95.6	95.6	94.7	94.1	93.1	91.7
27:TR: CompOut	167.8	167.3	166.7	166.2	166.3	166.5	165.1	164.4	163.4	162.0
28:TS: CompOut	121.5	121.1	120.7	120.3	120.5	120.6	119.7	119.3	118.9	118.2
29:TR: CondOut	109.8	109.4	109.0	108.7	108.8	108.9	107.6	107.3	106.9	106.2
30:TS: CondOut	109.7	109.3	108.9	108.6	108.7	108.8	107.5	107.2	106.8	106.2
31:TS: MullionIn	109.9	109.5	109.0	108.8	108.9	109.0	107.7	107.4	107.0	106.3
32:TS: MullionOut	109.1	108.7	108.3	108.0	108.1	108.2	107.0	106.7	106.3	105.6
33:TR: LiqLineOut	104.3	104.1	104.0	104.1	105.1	106.2	104.7	105.6	106.0	105.4
34:TS: LiqLineOut	103.8	103.5	103.4	103.4	104.3	105.3	103.9	104.8	105.5	104.9
35:TS: EvapIn	20.2	19.9	19.4	18.9	18.7	18.5	17.1	16.3	15.2	13.2
36:TS: EvapBendIn	22.6	22.3	21.8	21.3	21.0	20.8	19.6	18.7	17.6	15.7
45:TS: EvapBendIn_Mid	19.8	19.4	18.9	18.5	18.4	18.2	16.3	15.5	14.3	12.4
37:TS: EvapBendMid	23.4	23.0	22.3	21.6	21.2	20.9	19.4	18.6	17.4	15.6
46:TS: EvapBendMid_Out	26.4	25.0	20.7	18.7	18.1	17.7	15.8	14.9	13.8	11.9
38:TS: EvapBendOut	43.8	43.9	43.5	42.9	40.6	36.4	38.9	18.6	15.6	13.6

39:TR: EvapOut	43.8	43.6	43.0	41.4	37.5	33.1	34.0	26.0	17.4	12.1
40:TS: EvapOut	45.3	45.2	44.6	43.3	39.7	35.7	36.6	29.6	21.4	13.5
41:TS: CompShiTop	140.1	139.7	139.2	138.8	138.9	139.2	138.0	137.5	136.8	135.8
42:TS: CompShiBtm	150.7	150.4	150.0	149.7	149.8	150.1	149.2	148.8	148.3	147.6
43:TS: CompShiUpStrm										
44:TS: CompShiDnStrm	134.8	134.5	134.0	133.6	133.7	133.6	133.0	132.5	131.9	131.0
Power1:InWallLeft	5.5	5.5	5.6	5.5	5.4	5.4	5.6	5.6	5.5	5.4
Power2:InWallRight	119.6	119.0	117.9	117.3	117.4	117.3	114.2	113.4	111.5	108.3
Power3:Frez	0.0	0.0	0.0	0.0	0.0	0.0	0.0	0.0	0.0	0.0
Power4:FFC	190.5	191.2	189.0	188.0	186.0	184.3	179.6	172.9	170.3	156.5
Power5:OutWall	114.8	114.0	113.2	112.4	112.4	112.8	110.2	108.6	107.0	103.7
1:Press:CondOut	168.8	167.6	166.5	165.5	165.4	165.6	162.9	161.8	160.4	158.2
2:D_P:Cond	7.8	7.8	7.5	7.5	7.4	7.5	6.9	6.8	6.5	6.0
3:D_P:LiqLine	1.0	1.2	1.2	1.2	1.3	1.4	1.5	1.5	1.6	1.5
4:Press:EvapOut	30.5	30.3	29.9	29.7	29.6	29.6	28.5	28.1	27.4	26.3
5:D_P:SucLine	0.5	0.5	0.5	0.5	0.5	0.5	0.4	0.4	0.4	0.4
6:Press:Chamber	14.7	14.7	14.7	14.7	14.7	14.7	14.7	14.7	14.7	14.7
Air Vol. Flow rate (cfm)	50.3	48.1	45.4	42.6	39.4	36.4	33.1	27.3	22.8	20.0
subcooling (F)	5.06	4.80	4.41	4.12	3.18	2.14	2.30	1.04	0.16	0.08
superheat (F)	27.62	27.89	27.71	26.58	22.77	18.41	20.93	13.61	6.06	2.74
COP	1.861	1.888	1.906	1.928	1.942	1.952	1.952	1.910	1.888	1.823
Cooling Cap. (W)	262.9	261.7	258.4	256.4	254.8	252.8	244.4	233.9	225.7	210.8
FFC Runtime Fraction	0.0562	0.0554	0.0552	0.0548	0.0555	0.0567	0.0563	0.0593	0.0616	0.0662
Day	13	13	14	14	14	14	14	15	15	15
Month	7	7	7	7	7	7	7	7	7	7
Year	1999	1999	1999	1999	1999	1999	1999	1999	1999	1999